European Journal of Medicinal Chemistry 187 (2020) 111978

Contents lists available at ScienceDirect

European Journal of Medicinal Chemistry

journal homepage: http://www.elsevier.com/locate/ejmech

Research paper

Hydrogen sulfide releasing oridonin derivatives induce apoptosis through extrinsic and intrinsic pathways

Haonan Li [a], Jiahui Mu [a], Jianan Sun [a], Shengtao Xu [b], Weiwei Liu [c], Fanxing Xu [c], Zhanlin Li [a], Jinyi Xu [b], Huiming Hua [a], Dahong Li [a, *]

[a] Key Laboratory of Structure-Based Drug Design & Discovery, Ministry of Education, School of Traditional Chinese Materia Medica, Shenyang Pharmaceutical University, 103 Wenhua Road, Shenyang, 110016, PR China
[b] State Key Laboratory of Natural Medicines, China Pharmaceutical University, 24 Tongjia Xiang, Nanjing, 210009, PR China
[c] Wuya College of Innovation, Shenyang Pharmaceutical University, 103 Wenhua Road, Shenyang, 110016, PR China

ARTICLE INFO

Article history:
Received 23 September 2019
Received in revised form
12 December 2019
Accepted 16 December 2019
Available online 19 December 2019

Keywords:
ent-kaurane
Oridonin
Hydrogen sulfide
Antiproliferative activity
Apoptosis

ABSTRACT

Hydrogen sulfide (H_2S) has been recognized as the third endogenous signaling gasotransmitter following nitric oxide (NO) and carbon monoxide (CO), and exhibits antiproliferative activity against several cancer cells. In order to stably and controllably release H_2S, H_2S donating compound (ADT-OH) was used in the present study and 18H_2S releasing natural *ent*-kaurane diterpenoid oridonin derivatives were designed and synthesized. Most derivatives showed more potent antiproliferative activities than oridonin against HepG2 and K562 cell lines, while they were lack of sensitivity to HCT-116 and B16 cells. In particular, **12b** showed the most potent antiproliferative activities against HepG2, HCT-116 and K562 cells with IC_{50} values of 2.57, 5.81 and 0.95 μM, respectively. Through cell cycle analysis, **12b** caused cell cycle arrest at S phase in K562 cells and G1 phase in HepG2 cells. In Hoechst 33258 staining assay, cell shrinkage and fragmentation of cell nuclei indicated apoptotic morphological changes. Considering the decline of mitochondrial membrane potential and changes in the levels of apoptosis-related proteins, **12b** was shown to induce apoptosis through extrinsic and intrinsic apoptosis pathways.

1. Introduction

Natural products have made great contributions to drug design. With the development of analytical techniques, more and more active ingredients were isolated and identified from herbal medicines, natural plants and their metabolites. Many novel structural skeletons were provided for drug discovery, and relatively complete quality control systems were also established [1–4]. Compared with combinatorial chemistry, natural products remain active in drug discovery due to their prominent biological activities, complex and diverse structures and distinctive stereogenic centers which could better combine with corresponding targets in vivo [5]. In the past three decades, the percentage of natural products or nature derived molecules has increased to 74% of all approved chemical entities in anticancer domain [6,7].

As a rich source of *ent*-kaurane diterpenoids (Fig. 1), the genus *Rabdosia* exhibits many biological activities, including anti-inflammatory, anticancer, antibacterial and antimutagenic activities [8–17]. Oridonin (**1**, Fig. 1), a natural *ent*-kaurane diterpenoid from *Rabdosia*, was first isolated and identified by Fujita et al., in 1970 [18]. Further in-depth studies on pharmacology showed potent anticancer effects t(8; 21) acute myeloid leukemic (AML) cells [19], human pancreatic cancer PANC-1 cells [20], human osteosarcoma cells [21], p53-mutated colorectal cancer cells [22], drug-resistant renal cell carcinoma (RCC) [23] and non-germinal center B cell-like subtype of diffuse large B cell lymphoma (non-GCB DLBCL) [24]. Although oridonin can be obtained commercially and shows cytotoxicity for many cancer cells, it deserves further structural modification due to its poor selectivity and low aqueous solubility [25]. SAR studies indicated that unsaturated cyclopentanone conjugated with extracyclic methylene was a pivotal structure for antiproliferative activity, while the activity slumped when cyclopentanone was cleaved or methylene was saturated [26]. Furthermore, 14-hydroxy of oridonin was a prominent structure modification site. Most 14-*O*-derivatives showed maintained or better antiproliferative activities toward several human cancer cells [27,28].

* Corresponding author.
E-mail address: lidahong0203@163.com (D. Li).

https://doi.org/10.1016/j.ejmech.2019.111978
0223-5234/

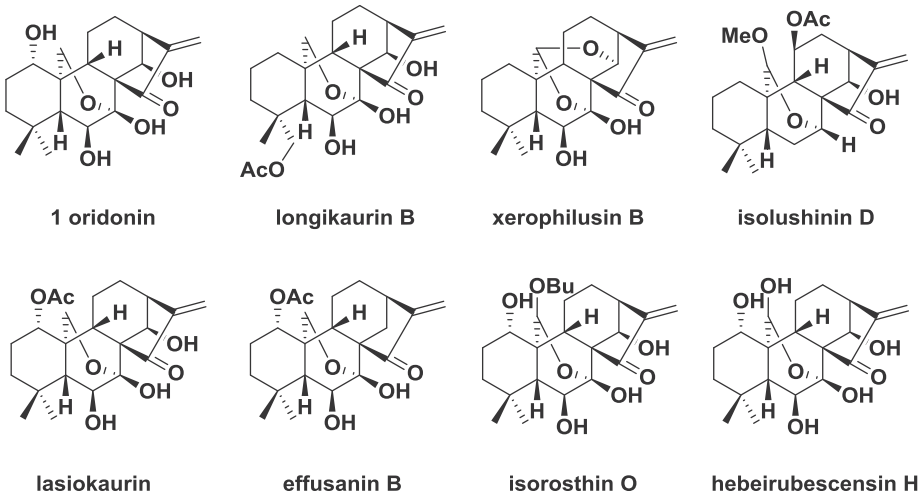

Fig. 1. The structures of natural *ent*-kaurane diterpenoids.

Due to the endogenous pathophysiological functions, small molecule donors have comprised a key pillar of drug design [29,30]. Before nitric oxide (NO) and carbon monoxide (CO) were famous for endogenous bioactivity, hydrogen sulfide (H_2S) was considered to be a colorless and toxic gas with a strong smell of rotten eggs. In recent years, it has been recognized as the third endogenous signaling gasotransmitter following NO and CO, acting as a neuromodulator and neuroprotective agent [31,32]. Endogenous H_2S commonly generates through two specific pyridoxal-5′-phosphate (PLP)-dependent enzymes, cystathionine-γ-lyase (CSE) and cystathionine-β-synthase (CBS), or biosynthesized by the synergistic effects of 3-mercaptopyruvate sulfurtransferase (3-MST) and cysteine aminotransferase (CAT) [33–35]. Increasing evidences confirm the pathophysiological functions of H_2S in atherosclerosis, cytoprotection against oxidative stress, angiogenesis, ischemia-reperfusion injury and so on [36–40]. In addition, recent studies demonstrate the importance of H_2S in biological processes of cancer which shows antiproliferative activities through EGFR/ERK/MMP-2, PTEN/AKT, PI3K/Akt/mTOR and p38 MAPK/ERK1/2-COX-2 pathways [41–44]. This reactivation of programmed cell death by delivery of H_2S could be suggested as an effective approach for cancer therapy. However, H_2S is not suitable for clinical applications directly owing to uncontrollability, high toxicity and short half-life. To overcome these disadvantages, a number of H_2S releasing agents (H_2S donors) have been developed, such as ADT-OH, thiobenzamide, Jks, *L*-propargyl cysteine, α-thioctic acid, GYY4137, DATS, D-cysteine and so on (Fig. 2A). These H_2S donating compounds could deliver H_2S in sustained manner and prolong the term of treating times [45–49]. With the development of H_2S donors, more and more H_2S releasing derivatives have been designed and synthesized. Some of them have entered into Phase I or Phase II clinical trials [[50–55], Fig. 2C]. Among them, compounds with 3*H*-1,2-dithiole-3-thione show prominent cytoprotective properties [[56], Fig. 2B].

In the present study, we designed and synthesized three series of H_2S releasing oridonin derivatives in which oridonin was conjugated with a H_2S generating moiety (5-(4-hydroxyphenyl)-3*H*-1,2-dithiole-3-thione, ADT-OH) via different anhydride linkers at 14-hydroxyl group. The antiproliferative activities of all the derivatives were tested against five human cancer cell lines (human hepatoma HepG2, breast cancer MCF-7, colorectal cancer HCT-116, melanoma B16 and chronic myelogenous leukemia K562) and two normal cell lines (human liver L-02 and peripheral blood mononuclear PBMC). Moreover, in-depth apoptosis related mechanisms of the most promising compound **12b** which included cell cycle arrest, morphological change, apoptosis induction, mitochondria membrane potentials decline and the expression of apoptosis-related proteins were studied.

2. Result and discussion

2.1. Chemistry

The intermediates **2** and **5** were synthesized according to our previous report [57]. The H_2S donating derivatives **7a-c** were obtained by substitution reactions of ADT-OH **6** with several bromhydrins (2-bromoethanol, 3-bromo-1-propanol and 6-bromo-1-hexanol). By treatment of **1**, **2** and **5** with corresponding anhydride in the presence of TEA/DMAP, derivatives **8a-c** and **9a-c** were got. Derivatives **8a-c** and **9a-c** were directly reacted with H_2S releasing **7a-c** via esterification reaction to gain the target compounds **10a-c**, **11a-c**, **12a-c**, **13a-c**, **14a-c** and **15a-c**. Among them, compounds **12c** and **15c** were dimeric diterpenoid compounds. The dimerization phenomenon would be due to the residual 6-bromo-1-hexanol after silica column chromatography (see Schemes 1 and 2).

2.2. Biological evaluation

2.2.1. Antiproliferative activity and preliminary SAR

MTT assay and trypan blue assay were performed to evaluate the antiproliferative activities of 18 synthetic derivatives (**10a-c**, **11a-c**, **12a-c**, **13a-c**, **14a-c** and **15a-c**), lead compound oridonin (**1**) and H_2S donor ADT-OH (**6**). The IC_{50} values against five human cancer cells (HepG2, MCF-7, HCT-116, B16 and K562) and two human normal cells (L-02 and PBMC) were calculated and listed in Table 1. Although the antiproliferative activities of most derivatives were more potent than oridonin in HepG2 and K562 cell lines, they were lack of sensitivity to HCT-116 and B16 cells. Only **12b** was stronger than oridonin with IC_{50} values of 5.81 and 12.94 μM, while exhibited only appropriate effect in MCF-7 cell line (16.15 μM) which was similar to that of oridonin (13.85 μM). In HepG2 and K562 cells, compared with compounds containing carbonyl or hydroxyl group at C-1, acetylated derivatives (**10**–**15b**) usually possessed more potent cytotoxicity, their IC_{50} values were universally below 6 μM. Furthermore, acetylated derivatives which

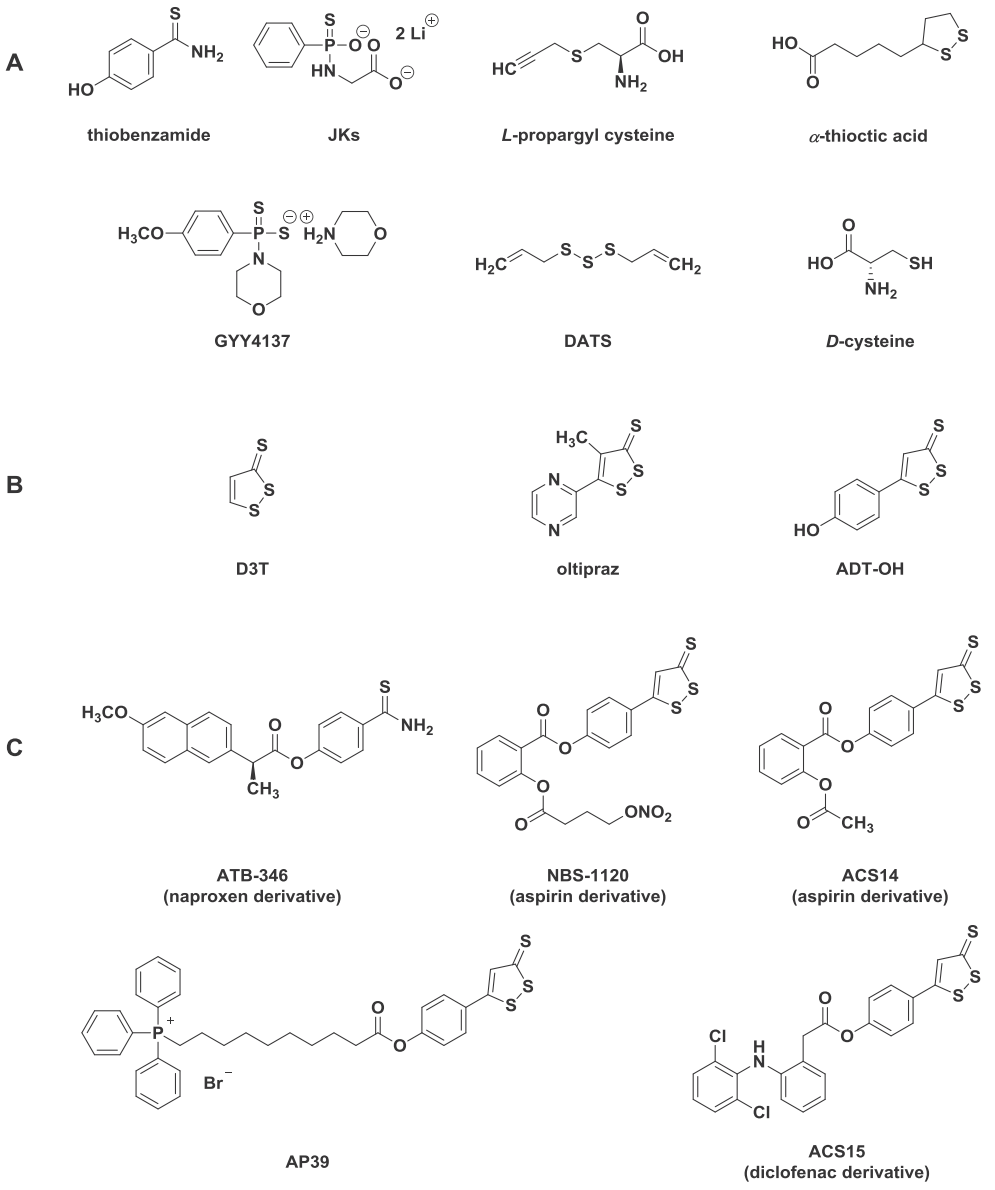

Fig. 2. The structures of H_2S donors (A), compounds with 3*H*-1,2-dithiole-3-thione group (B) and H_2S releasing drug candidates (C).

conjugated with succinic anhydride as a linker (**10**–**12b**) were stronger than those with glutaric anhydride (**13**–**15b**). However, it will no longer be in line with this trend when acetyl group changed to carbonyl or hydroxyl group at C-1. Comprehensive analysis of antiproliferative data in HepG2, MCF-7 and K562 cells indicated that more efficacious inhibitory activities were not observed with the extension of carbon chain. It seemed that compounds with medium-length carbon chains ($n_2 = 3$) showed better antiproliferative activities in general, yet compound **12b** with long carbon chains ($n_2 = 6$) still exhibited the most potent antiproliferative activity in all derivatives against HepG2, HCT-116 and K562 cells with IC_{50} values of 2.57, 5.81 and 0.95 μM, respectively.

Cultivated with 18 derivatives, the cell viability of L-02 and PBMC cells was not significantly affected which indicated good selectivity of inhibitory activity between tumor and normal cells. Besides efficacious antiproliferative activity, **12b** also showed nearly 20-fold lower inhibitory activities against L-02 and PBMC cells than those of malignant cells.

2.2.2. H_2S release ability

In order to observe H_2S generation capability of all hybrids, the methylene blue (MB^+) method was carried out and H_2S-releasing curves were calculated and summarized in Fig. 3. The delivery of H_2S elevated as time increased and reached the peak value at 15 or 20 min, indicating all H_2S-donating compounds could release H_2S in a relatively slow manner. Considering the cytotoxicity and potential SAR of the derivatives, it did not seem that the more H_2S released, the better inhibitory activity exhibited. Compounds contained a hydroxyl group at C-1 (**10**–**12c**, **14c** and **15c**) showed higher H_2S releasing capacity (15–20 μM) when compared with 1-acetylated and 1-oxo derivatives. Furthermore, the length of n_1 and n_2 also seemed to be another decisive factor to the release of H_2S. With the increased length of carbon chains, higher H_2S release was observed. It seemed that a certain amount of H_2S was sufficient for antiproliferative treatments.

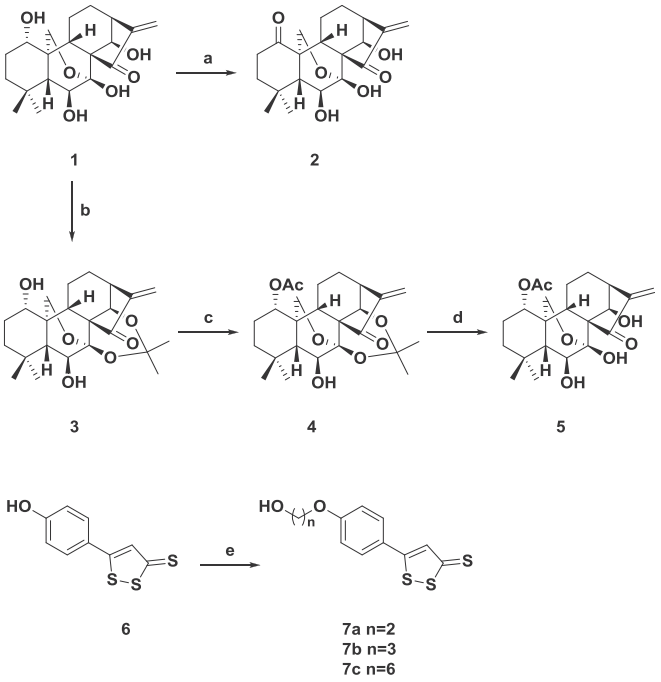

Scheme 1. Synthetic routes of the intermediates. Reagents and conditions: (a) Jones reagent, acetone, 0 °C, 0.5 h; (b) 2,2-dimethoxypropane, acetone, TsOH, reflux, 2 h; (c) Ac_2O, TEA, DMAP, DCM, rt, 5 h; (d) 10% HCl, THF, rt, 4 h; (e) correspondent bromoalcohol, K_2CO_3, acetone, reflux, 6 h.

2.2.3. ***12b*** *caused cell cycle arrest at S phase in K562 cells and G1 phase in HepG2 cells*

Cell cycle plays an important role in cell life activities due to its regulation of division and duplication of DNA. Dysregulation of cell cycle may contribute to persistent tumor cell proliferation. Considering many anticancer compounds showed cytotoxicity which was associated with cell cycle arrest at a particular checkpoint, the influence of **12b** to cell cycle arrest was analyzed and DNA content of cell nuclei which stained by propidium iodide (PI) was monitored by flow cytometry. As shown in Fig. 4A–B, **12b** arrested K562 cell cycle at S phase and HepG2 cell at G1 phase. In contrast, oridonin caused cell cycle arrest of K562 and HepG2 cells both at G1 phase. In short, **12b**-mediated cell cycle arrest could be responsible for the inhibition of tumor cell proliferation.

2.2.4. *Hoechst 33258 staining indicated that* ***12b*** *induced pyknosis in K562 cells*

Apoptosis is prescribed as the major killing way of tumor cells after antitumor drugs treatment. Hence, we verified whether **12b** induces K562 cell apoptosis. The occurrence of apoptosis usually concomitant of deviant morphological characteristics included cell shrinkage, chromatin condensation, cell membrane rupture and fragmentation of cell nuclei [58]. In order to preliminarily verify the occurrence of apoptosis, Hoechst 33258 staining assay and fluorescence microscope were used to observe the morphology of aberrant. Three random microscopic fields per sample of approximately 200 nuclei were counted and expressed as the percentage of apoptotic nuclei in histogram. As shown in Fig. 5, compared with vehicle control (DMSO), some fragment could be observed in K562 cells incubated with **12b** (1.0, 2.0 and 4.0 μM) for 24 h and 48 h, demonstrating the occurrence of chromatin shrink and nuclear fragmentation, and showed obvious concentration dependence.

2.2.5. *Flow cytometric analysis suggested that* ***12b*** *induced apoptosis in K562 and HepG2 cells*

Apoptosis is essential to multicellular organisms development, it will be triggered when a cell commits suicide. Apoptosis is also referred to programmed cell death and follows a controlled predictable routine, while cancer cells can suppress apoptosis and proliferate incessantly. Hence, great efforts have been exerted to induce cancer cells apoptosis by developing chemical entities. To evaluate the effects of **12b** on induction of apoptosis and quantify the percentage of apoptotic cells, an annexin V-FITC/PI binding assay was carried out. Cultivated with **12b** (0, 0.50, 1.0 and 2.0 μM), the percentage of K562 and HepG2 cells underwent apoptosis which was tested via flow cytometry. As shown in Fig. 6, apoptotic ratios of K562 and HepG2 cells (annexin V^+) obviously increased in a concentration-dependent manner. Consequently, **12b** was capable of inducing apoptosis both in K562 and HepG2 cells.

2.2.6. ***12b*** *induced mitochondrial membrane potentials decline*

The decline of mitochondrial membrane potentials is known as the classic characteristics of early apoptosis process, which is also critical to the apoptotic pathway. To ensure mitochondrial integrity and biological function, the maintenance of mitochondrial

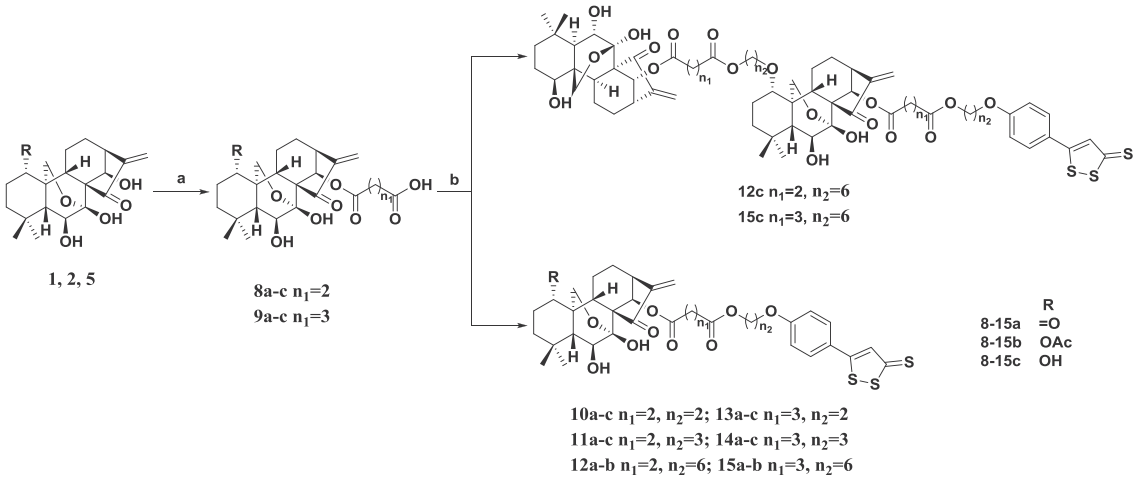

Scheme 2. Synthesis of H_2S donating derivatives **10a-c**, **11a-c**, **12a-c**, **13a-c**, **14a-c** and **15a-c**. Reagents and conditions: (a) correspondent anhydride, TEA, DMAP, DCM, rt, 7 h; (b) **7a-c**, EDCI, DMAP, DCM, rt, overnight.

Table 1
Antiproliferative activities (IC50[a] μM) of 18 target derivatives, parental compounds and H_2S donors against five human cancer and two normal cell lines.

Compd.	IC50 (μM)						
	HepG2	MCF-7	HCT-116	B16	K562	L-02	PBMC
1	8.95 ± 0.68	13.85 ± 1.23	11.73 ± 1.01	24.89 ± 1.32	4.57 ± 0.20	21.59 ± 1.46	>50
2	10.51 ± 0.73	15.39 ± 1.50	10.67 ± 0.75	25.46 ± 1.08	4.17 ± 0.17	28.54 ± 1.31	>50
5	11.94 ± 1.02	19.82 ± 1.36	13.48 ± 0.86	32.57 ± 1.33	5.21 ± 0.19	25.39 ± 1.78	>50
6	>50	>50	>50	>50	>50	>50	>50
10a	7.52 ± 0.72	25.44 ± 1.23	>50	>50	8.79 ± 0.21	39.64 ± 1.20	>50
11a	5.01 ± 0.26	19.52 ± 1.30	13.97 ± 0.71	>50	7.12 ± 0.33	>50	>50
12a	10.47 ± 0.73	34.80 ± 2.56	>50	>50	5.87 ± 0.43	>50	>50
13a	7.65 ± 0.57	27.51 ± 1.64	34.88 ± 1.59	>50	5.75 ± 0.12	42.16 ± 1.58	>50
14a	2.58 ± 0.20	12.47 ± 1.03	23.70 ± 1.51	39.94 ± 1.61	3.59 ± 0.09	27.18 ± 1.72	>50
15a	9.33 ± 0.65	>50	>50	>50	8.89 ± 0.25	>50	>50
10b	5.89 ± 0.36	24.72 ± 1.53	36.85 ± 1.54	>50	2.85 ± 0.10	29.93 ± 1.38	>50
11b	6.30 ± 0.58	20.81 ± 1.37	22.06 ± 1.41	16.38 ± 1.25	2.44 ± 0.13	22.31 ± 1.72	>50
12b	2.57 ± 0.12	16.15 ± 1.02	5.81 ± 1.17	12.94 ± 0.88	0.95 ± 0.06	17.59 ± 0.93	>50
13b	4.78 ± 0.40	>50	>50	11.09 ± 0.86	1.86 ± 0.15	26.84 ± 1.40	>50
14b	3.57 ± 0.31	15.75 ± 1.23	37.47 ± 1.66	>50	5.93 ± 0.18	33.51 ± 1.85	>50
15b	15.60 ± 1.52	>50	>50	>50	13.88 ± 0.46	>50	>50
10c	5.36 ± 0.28	17.86 ± 1.35	42.61 ± 2.95	>50	4.57 ± 0.21	33.96 ± 2.55	>50
11c	4.45 ± 0.34	14.67 ± 1.21	27.48 ± 1.60	27.50 ± 0.92	2.17 ± 0.15	26.54 ± 1.70	>50
12c	12.26 ± 1.04	>50	>50	>50	14.86 ± 0.94	>50	>50
13c	6.60 ± 0.53	18.30 ± 1.42	38.35 ± 2.26	>50	4.89 ± 0.34	39.11 ± 1.42	>50
14c	5.93 ± 0.47	16.63 ± 1.35	34.16 ± 1.73	>50	4.19 ± 0.22	40.92 ± 1.77	>50
15c	10.05 ± 0.55	>50	>50	>50	13.47 ± 0.68	>50	>50
5-Fu	32.57 ± 1.98	26.65 ± 1.92	6.86 ± 0.37	12.62 ± 1.06	3.94 ± 0.17	>50	>50

[a]IC_{50}: Half inhibitory concentrations measured by the MTT assay and trypan blue assay. The values are expressed as averages ± standard deviations of three independent experiments.

membrane potentials is crucial [59]. Cells pretreated with **12b** (0.50, 1.0 and 2.0 μM) or DMSO (vehicle control) were stained with the lipophilic cationic fluorescent probe 5,5′,6,6′-tetrachloro-1,1′,3,3′-tetraethylbenzimidazol-carbocyanine iodide (JC-1), and then the effects of **12b** on mitochondrial membrane potentials were detected by flow cytometry. As shown in Fig. 7A and B, mitochondrial membrane potentials of K562 and HepG2 cells treated with **12b** was significantly decreased in a concentration-dependent manner. These results indicated that **12b** influenced the permeability of mitochondrial membrane and eventually led to apoptosis.

*2.2.7. **12b** treatment activated extrinsic and intrinsic apoptosis pathways followed by regulation of apoptosis-related protein levels*

Apoptosis is a process of autonomous cell death that is strictly controlled by multiple genes, which plays an important role in the evolution of organisms, the homeostasis of internal environment and the development of multiple systems. Extrinsic and intrinsic apoptosis pathways generally mediate by several apoptosis related proteins. When the expression of Bax, Bcl-2 and other factors changes, the opening of permeability transition pore on outer mitochondrial membrane will be triggered which concomitantly delivers cytochrome *c*. Once cytochrome *c* releases into outer cytoplasm, it will form apoptotic bodies with Apaf-1 and then activate downstream apoptotic protein caspase-9. Activated caspase-9 then cleaves downstream procaspase-3 to cut it into active for activated caspase-3 immediately. Finally, caspase-3 causes the execution of intrinsic apoptosis by cleaving targeted cellular proteins. IAPs (Inhibitor of apoptosis proteins) are a group of apoptotic regulatory proteins which mediate intracellular or extracellular apoptosis pathways by inhibiting caspase activity directly or indirectly, or preventing the release of mitochondrial apoptotic precursors. Up to now, eight apoptotic inhibitory proteins have been found: c-IAP1, c-IAP2, NAIP, Survivin, XIAP, Bruce, ILP-2 and Livin. The activation of caspase family can be inhibited by c-IAPs, Survivin and XIAP through BIR structural domain. Hence, inhibiting IAPs is one of the most effective method to prevent tumorigenesis [60]. Moreover, TRAIL induces apoptosis mainly by binding to DR4 and DR5 death receptors [61]. The higher binding level of DR4/DR5 to TRAIL, the more apoptosis would be observed.

To analyze the mediative mechanism of **12b** on apoptosis, the Human Apoptosis Array kit was used to detect the relative expression of 35 apoptosis-related proteins. Each dot represents which antibodies were shown in the Human Apoptosis Array coordinates (Fig. S1), and the original image of Human Apoptosis Array kit was shown in Fig. S2. As shown in Fig. 8, the down-regulated level of procaspase-3 and the increase in cleaved caspase-3 demonstrated that **12b** could trigger caspase-dependent apoptosis pathway. Furthermore, the level of pro-apoptotic protein Bax was elevated after the treatment with **12b** (1 μM) for 24 h, suggesting the participation of the endogenous apoptosis pathway. Compared with the control group, the protein levels of c-IAP1, c-IAP2, Survivin, XIAP and Livin were significantly decreased. Hence, we reasoned that **12b** could inhibit the expression of related proteins in IAPs to ensure the activation of caspase pathway and ultimately induce apoptosis through mitochondria-dependent intrinsic pathway. Furthermore, the expressions of DR4 and DR5 were found to be elevated compared with the control group, indicating the extrinsic apoptotic pathway would also be associated with apoptosis induced by **12b** (Fig. 9).

3. Conclusion

Overall, by using oridonin as lead compound, we designed and synthesized 18H_2S-delivering derivatives in the present study. Five tumor and two normal cell lines were selected to test the antiproliferative activities of all derivatives. Most derivatives were sensitive to HepG2 and K562 cells and several compounds showed improved effects than parent compound oridonin. In particular, **12b** not only showed the most potent antiproliferative activities against HepG2, HCT-116 and K562 cells with IC_{50} values of 2.57, 5.81 and 0.95 μM respectively, but also exhibited lower toxicity to two human normal cells. Further in-depth cellular mechanism exploration showed that **12b** caused cell cycle arrest at S phase in K562 cells and G1 phase in HepG2 cells. **12b** also reduced mitochondrial

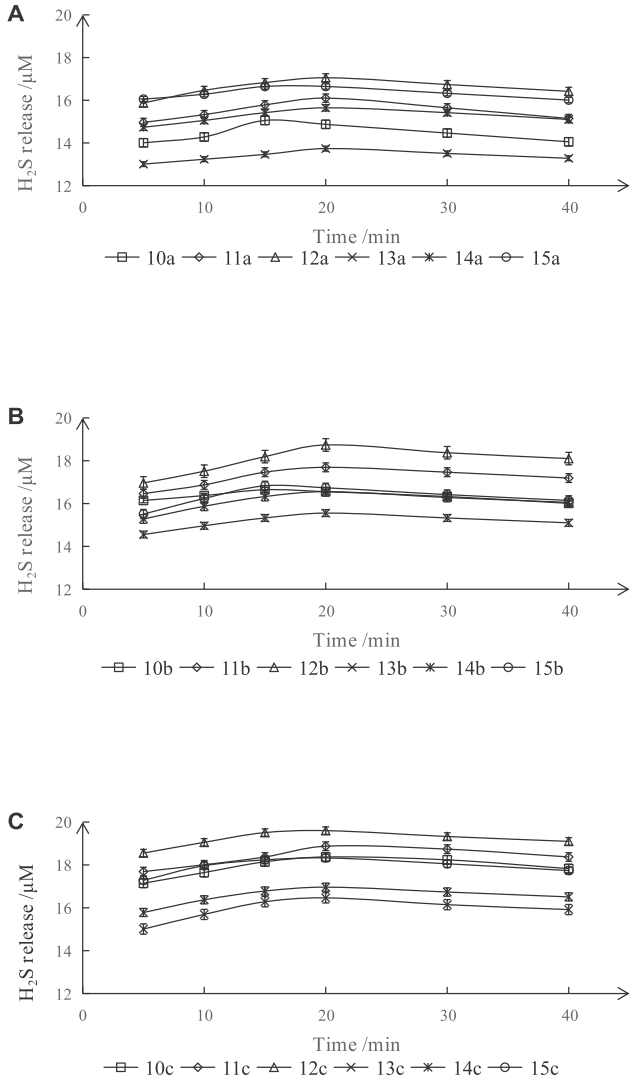

Fig. 3. In vitro H_2S release of **10**–**15a** (A), **10**–**15b** (B) and **10**–**15c** (C) at a dose of 0.1 mM using TCEP as accelerator. The absorbance of each resulting mixture was detected by UV–Vis spectrometer (670 nm). The amount of H_2S was calculated through the Na_2S standard curve. All of the data were the mean ± SD of three independent tests.

membrane potentials in both K562 and HepG2 cells and affected apoptosis-related proteins through extrinsic and intrinsic pathways. In conclusion, **12b** with potent antiproliferative activities, deserved further investigation as a potential anticancer candidate.

4. Experimental

4.1. Chemistry

Chemical materials and reagents were obtained from commercial suppliers, the preparation of anhydrous solvents was based on standard methods. ^{1}H and ^{13}C NMR spectra were determined with Bruker 400 MHz spectrometer in the solvent of $CDCl_3$ (TMS as internal standard): the values of the chemical shifts were reported in δ values (ppm) and the coupling constants (J) in Hz. High resolution mass spectra (HR-MS) were analyzed on Agilent Q-TOF B.05.01 (B5125.2).

4.1.1. General procedures to synthesize target derivatives

1-oxo intermediate **2**, acetylated derivative **5** and ADT-OH **6** were synthesized according to our previous report [57]. Correspondent bromoalcohol was added into anhydrous acetone in the presence of sodium carbonate and ADT-OH **6**. After reflux for 8 h, the reaction mixture was filtered and washed with acetone, and then the filtrate was evaporated in vacuo, the crude product was purified by silica column chromatography (PE/EA 4:1, v/v) to yield **7a-c**.

Compounds **1**, **2** or **5** (0.50 mmol) were dissolved in 6 mL anhydrous DCM in the presence of TEA (2.5 mmol), DMAP (0.25 mmol) and succinic anhydride or glutaric anhydride (1.0 mmol) and stirred at room temperature for 6–8 h. The mixture was extracted with DCM (3 × 20 mL), washed with brine, dried over anhydrous Na_2SO_4, and evaporated in vacuo to yield intermediates **8a-c** and **9a-c**. Intermediates **10a-c** or **15a-c** (0.20 mmol) were dissolved in anhydrous DCM and directly reacted with **7a-c** (0.22 mmol) under the condition of EDCI (0.60 mmol) and DMAP (0.10 mmol). After stirring overnight at room temperature, the reaction was quenched and extracted with DCM (3 × 20 mL), washed with brine, dried over anhydrous Na_2SO_4, and evaporated in vacuo. Finally, H_2S-releasing derivatives **10a-c**, **11a-c**, **12a-c**, **13a-c**, **14a-c** and **15a-c** were obtained by flash column chromatography (DCM/MeOH 100:1–200:1, v/v).

4.1.1.1. Compound ***10a***.

(4a*R*,5*S*,6*S*,6a*R*,9*S*,11a*S*,11b*S*,14*R*)-5,6-dihydroxy-4,4-dimethyl-8-methylene-1,7-dioxododecahydro-1*H*-6,11b-(epoxymethano)-6a,9-methanocyclohepta[*a*]naphthalen-14-yl(2-(4-(3-thioxo-3*H*-1,2-dithiol-5-yl)phenoxy)ethyl) succinate. Orange red solid, yield: 37.6%, m.p. 57–59 °C. ^{1}H NMR ($CDCl_3$, 400 MHz), δ (ppm): 7.63, 7.00 (each 2H, d, $J_A = J_B = 8.8$ Hz, Ar–H), 7.40 (1H, s, 8″-CH), 6.25 (1H, s, 17-CH_2), 5.93 (1H, s, 14-CH), 5.62 (1H, s, 17-CH_2), 5.36 (1H, d, $J = 11.9$ Hz, 6-OH), 4.46 (2H, dd, $J = 9.6$, 4.7 Hz, 5′-CH_2), 4.23 (2H, t, $J = 4.7$ Hz, 6′-CH_2), 4.29, 4.01 (each 1H, d, $J = 10.7$ Hz, 20-CH_2), 3.75 (1H, dd, $J = 11.7$, 8.9 Hz, 6-CH), 3.10 (1H, d, $J = 9.4$ Hz, 13-CH), 2.69 (2H, m, 3′-CH_2), 2.58 (2H, m, 2′-CH_2), 2.54–2.41 (2H, m, $-CH_2$), 2.33, 2.20 (each 1H, m, $-CH_2$), 1.93 (2H, m, $-CH_2$), 1.77–1.57 (4H, m, $-CH_2$), 1.31 (2H, m, $-CH_2$), 1.19 (3H, s, 18-CH_3), 0.98 (3H, s, 19-CH_3); ^{13}C NMR ($CDCl_3$, 100 MHz), δ (ppm): 215.48, 211.51, 204.79, 172.09, 170.82, 161.93, 149.50, 134.83, 128.62 (× 2), 122.08, 115.61 (× 2), 96.85, 74.50, 73.39, 66.13, 64.92, 62.73, 61.32, 59.75, 50.73, 48.54, 41.47, 38.38, 35.73, 32.85, 30.51, 30.05, 29.49, 28.83, 23.17, 19.17; HRMS (ESI) m/z calcd for $C_{35}H_{38}O_{10}S_3$ $[M - H]^-$ 713.1549, found 713.1566.

4.1.1.2. Compound ***11a***.

(4a*R*,5*S*,6*S*,6a*R*,9*S*,11a*S*,11b*S*,14*R*)-5,6-dihydroxy-4,4-dimethyl-8-methylene-1,7-dioxododecahydro-1*H*-6,11b-(epoxymethano)-6a,9-methanocyclohepta[*a*]naphthalen-14-yl(3-(4-(3-thioxo-3*H*-1,2-dithiol-5-yl)phenoxy)propyl) succinate. Orange red solid, yield: 36.2%, m.p. 60–62 °C. ^{1}H NMR ($CDCl_3$, 400 MHz), δ (ppm): 7.62, 6.98 (each 2H, d, $J_A = J_B = 8.7$ Hz, Ar–H), 7.39 (1H, s, 8″-CH), 6.24 (1H, s, 17-CH_2), 5.92 (1H, s, 14-CH), 5.62 (1H, s, 17-CH_2), 5.37 (1H, d, $J = 11.3$ Hz, 6-OH), 4.31–4.25 (3H, m, 5′-CH_2, 20-CH_2), 4.10 (2H, t, $J = 6.1$ Hz, 7′-CH_2), 4.01 (1H, d, $J = 10.7$ Hz, 20-CH_2), 3.76 (1H, m, 6-CH), 3.09 (1H, d, $J = 9.4$ Hz, 13-CH), 2.61 (2H, m, 3′-CH_2), 2.58 (2H, m, 2′-CH_2), 2.53–2.40 (2H, m, $-CH_2$), 2.33, 2.20 (each 1H, m, $-CH_2$), 2.13 (2H, t, $J = 6.1$ Hz, 2′-CH_2), 1.93 (2H, m, $-CH_2$), 1.76–1.56 (4H, m, $-CH_2$), 1.31 (2H, m, $-CH_2$), 1.19 (3H, s, 18-CH_3), 0.98 (3H, s, 19-CH_3); ^{13}C NMR ($CDCl_3$, 100 MHz), δ (ppm): 215.17, 211.52, 204.79, 172.99, 172.14, 170.92, 162.13, 149.48, 134.68, 128.62 (× 2), 124.31, 122.08, 115.49 (× 2), 96.86, 74.51, 73.39, 64.92, 64.82, 61.42, 61.32, 59.78, 50.73, 48.54, 41.46, 38.39, 35.74, 32.86, 30.51, 30.04, 29.53, 28.87, 28.42, 23.18, 19.16; HRMS (ESI) m/z calcd for $C_{36}H_{40}O_{10}S_3$ $[M - H]^-$

727.1706, found 727.1711.

4.1.1.3. Compound **12a**.

(4a*R*,5*S*,6*S*,6a*R*,9*S*,11a*S*,11b*S*,14*R*)-5,6-dihydroxy-4,4-dimethyl-8-methylene-1,7-dioxododecahydro-1*H*-6,11b-(epoxymethano)-6a,9-methanocyclohepta[*a*]naphthalen-14-yl(6-(4-(3-thioxo-3*H*-1,2-dithiol-5-yl)phenoxy)hexyl) succinate. Orange red solid, yield: 31.2%, m.p. 65–67 °C. ^{1}H NMR ($CDCl_3$, 400 MHz), δ (ppm): 7.61, 6.96 (each 2H, d, $J_A = J_B = 8.7$ Hz, Ar–H), 7.40 (1H, s, 8″-CH), 6.25 (1H, s, 17-CH_2), 5.92 (1H, s, 14-CH), 5.62 (1H, s, 17-CH_2), 5.38 (1H, d, $J = 11.1$ Hz, 6-OH), 4.29 (1H, d, $J = 10.7$ Hz, 20-CH_2), 4.08 (2H, m, 5′-CH_2), 4.05–3.99 (3H, m, 10′-CH_2, 20-CH_2), 3.77 (1H, t, $J = 9.4$ Hz, 6-CH), 3.10 (1H, d, $J = 9.4$ Hz, 13-CH), 2.59 (2H, m, 2′-CH_2), 2.55 (2H, m, 3′-CH_2), 2.52–2.40 (2H, m, –CH_2), 2.33, 2.21 (each 1H, m, –CH_2), 1.94 (2H, m, –CH_2), 1.89–1.56 (10H, m, –CH_2), 1.31 (2H, m, –CH_2), 1.19 (3H, s, 18-CH_3), 0.99 (3H, s, 19-CH_3); ^{13}C NMR ($CDCl_3$, 100 MHz), δ (ppm): 215.08, 211.57, 204.80, 173.15, 172.26, 170.99, 162.52, 149.49, 134.58, 129.21, 128.60 (× 2), 124.03, 122.04, 115.47 (× 2), 96.86, 74.56, 73.36, 66.24, 64.92, 64.78, 61.31, 59.83, 50.77, 48.56, 41.45, 38.42, 35.76, 32.86, 30.51, 30.04, 29.69, 29.57, 28.92, 28.46, 25.63, 23.20, 19.16; HRMS (ESI) *m*/*z* calcd for $C_{39}H_{46}O_{10}S_3$ $[M - H]^-$ 769.2175, found 769.2182.

4.1.1.4. Compound **13a**.

(4a*R*,5*S*,6*S*,6a*R*,9*S*,11a*S*,11b*S*,14*R*)-5,6-dihydroxy-4,4-dimethyl-8-methylene-1,7-dioxododecahydro-1*H*-6,11b-(epoxymethano)-6a,9-methanocyclohepta[*a*]naphthalen-14-yl(2-(4-(3-thioxo-3*H*-1,2-dithiol-5-yl)phenoxy)ethyl) glutarate. Orange red solid, yield: 28.4%, m.p. 59–61 °C. ^{1}H NMR ($CDCl_3$, 400 MHz), δ (ppm): 7.62, 6.98 (each 2H, d, $J_A = J_B = 8.8$ Hz, Ar–H), 7.39 (1H, s, 8″-H), 6.23 (1H, s, 17-CH_2), 5.90 (1H, s, 14-CH), 5.60 (1H, s, 17-CH_2), 5.35 (1H, d, $J = 11.6$ Hz, 6-OH), 4.44 (2H, t, $J = 4.8$ Hz, 6′-CH_2), 4.28, 4.01 (each 1H, d, $J = 10.6$ Hz, 20-CH_2), 4.22 (2H, t, $J = 4.8$ Hz, 7′-CH_2), 4.06 (1H, brs, –OH), 3.74 (1H, dd, $J = 10.8$, 9.0 Hz, 6-CH), 3.08 (1H, d, $J = 9.3$ Hz, 13-CH), 2.59–2.42 (2H, m, 3′-CH_2), 2.39 (2H, t, $J = 7.2$ Hz, 4′-CH_2), 2.32 (2H, t, $J = 7.2$ Hz, 2′-CH_2), 2.20 (1H, dd, $J = 13.7$, 4.6 Hz, –CH_2), 1.93 (2H, m, –CH_2), 1.72, 1.61 (each 1H, m, –CH_2), 1.31 (2H, m, –CH_2), 1.18 (3H, s, 18-CH_3), 0.98 (3H, s, 19-CH_3); ^{13}C NMR ($CDCl_3$, 100 MHz), δ (ppm): 215.20, 211.48, 204.81, 172.80, 172.70, 171.33, 161.74, 149.50, 134.80, 128.65 (× 2), 124.66, 122.00, 115.58 (× 2), 96.85, 74.37, 73.33, 66.17, 64.93, 62.33, 61.30, 59.81, 50.71, 48.55, 41.51, 38.40, 35.75, 33.38, 32.92, 32.84, 30.51, 30.05, 23.17, 19.67, 19.14; HRMS (ESI) *m*/*z* calcd for $C_{36}H_{40}O_{10}S_3$ $[M - H]^-$ 727.1706, found 727.1691.

4.1.1.5. Compound **14a**.

(4a*R*,5*S*,6*S*,6a*R*,9*S*,11a*S*,11b*S*,14*R*)-5,6-dihydroxy-4,4-dimethyl-8-methylene-1,7-dioxododecahydro-1*H*-6,11b-(epoxymethano)-6a,9-methanocyclohepta[*a*]naphthalen-14-yl(3-(4-(3-thioxo-3*H*-1,2-dithiol-5-yl)phenoxy)propyl) glutarate. Orange red solid, yield: 25.5%, m.p. 62–63 °C. ^{1}H NMR ($CDCl_3$, 400 MHz), δ (ppm): 7.61, 6.97 (each 2H, d, $J_A = J_B = 8.7$ Hz, Ar–H), 7.39 (1H, s, 8″-H), 6.24 (1H, s, 17-CH_2), 5.90 (1H, s, 14-CH), 5.61 (1H, s, 17-CH_2), 5.37 (1H, d, $J = 11.6$ Hz, 6-OH), 4.31–4.24 (3H, m, 6′-CH_2, 20-CH_2), 4.10 (2H, t, $J = 6.2$ Hz, 8′-CH_2), 4.02 (1H, d, $J = 10.6$ Hz, 20-CH_2), 3.74 (1H, dd, $J = 11.5$, 9.0 Hz, 6-CH), 3.08 (1H, d, $J = 9.4$ Hz, 13-CH), 2.59–2.40 (2H, m, –CH_2), 2.37–2.29 (5H, m, –CH_2), 2.13 (2H, t, $J = 6.1$ Hz, 2′-CH_2), 1.90 (4H, m, –CH_2), 1.31 (2H, m, –CH_2), 1.18 (3H, s, 18-CH_3), 0.99 (3H, s, 19-CH_3); ^{13}C NMR ($CDCl_3$, 100 MHz), δ (ppm): 215.14, 211.47, 204.80, 172.99, 172.76, 171.34, 162.12, 149.49, 134.67, 128.62 (× 2), 124.31, 122.00, 115.48 (× 2), 96.92, 74.39, 73.33, 64.94, 64.83, 61.30, 61.03, 59.83, 50.71, 48.55, 41.50, 38.41, 35.75, 33.48, 33.05, 32.86, 30.52, 30.05, 28.46, 23.18, 19.74, 19.14; HRMS (ESI) *m*/*z* calcd for $C_{37}H_{42}O_{10}S_3$ $[M - H]^-$ 741.1862, found 741.1845.

4.1.1.6. Compound **15a**.

(4a*R*,5*S*,6*S*,6a*R*,9*S*,11a*S*,11b*S*,14*R*)-5,6-dihydroxy-4,4-dimethyl-8-methylene-1,7-dioxododecahydro-1*H*-6,11b-(epoxymethano)-6a,9-methanocyclohepta[*a*]naphthalen-14-yl(6-(4-(3-thioxo-3*H*-1,2-dithiol-5-yl)phenoxy)hexyl) glutarate. Orange red solid, yield: 34.2%, m.p. 69–70 °C. ^{1}H NMR ($CDCl_3$, 400 MHz), δ (ppm): 7.61, 6.96 (each 2H, d, $J_A = J_B = 8.7$ Hz, Ar–H), 7.40 (1H, s, 8″-H), 6.25 (1H, s, 17-CH_2), 5.90 (1H, s, 14-CH), 5.62 (1H, s, 17-CH_2), 5.37 (1H, d, $J = 11.7$ Hz, 6-OH), 4.30 (1H, d, $J = 10.6$ Hz, 20-CH_2), 4.08 (2H, t, $J = 6.7$ Hz, 6′-CH_2), 4.05–4.00 (3H, m, 11′-CH_2, 20-CH_2), 3.77 (1H, t, $J = 10.0$ Hz, 6-CH), 3.10 (1H, d, $J = 9.4$ Hz, 13-CH), 2.59 (2H, m, 2′-CH_2), 2.58–2.40 (2H, m, –CH_2), 2.21 (1H, dd, $J = 13.8$, 4.2 Hz, –CH_2), 1.99–1.78 (8H, m, –CH_2), 1.31 (2H, m, –CH_2), 1.19 (3H, s, 18-CH_3), 1.00 (3H, s, 19-CH_3); ^{13}C NMR ($CDCl_3$, 100 MHz), δ (ppm): 215.28, 211.51, 204.82, 172.89, 171.40, 162.51, 149.48, 134.57, 128.58 (× 2), 124.00, 121.98, 115.46 (× 2), 96.92, 74.47, 73.31, 68.26, 64.93, 64.38, 61.29, 59.89, 50.74, 48.57, 41.49, 38.44, 35.77, 33.53, 33.14, 32.86, 30.52, 30.05, 29.69, 28.93, 28.51, 25.64, 23.19, 22.67, 19.79, 19.13, 14.10; HRMS (ESI) *m*/*z* calcd for $C_{40}H_{48}O_{10}S_3$ $[M - H]^-$ 783.2332, found 783.2305.

4.1.1.7. Compound **10b**.

(1*S*,4a*R*,5*S*,6*S*,6a*R*,9*S*,11a*S*,11b*S*,14*R*)-1-acetoxy-5,6-dihydroxy-4,4-dimethyl-8-methylene-7-oxododecahydro-1*H*-6,11b-(epoxymethano)-6a,9-methanocyclohepta[*a*]naphthalen-14-yl(2-(4-(3-thioxo-3*H*-1,2-dithiol-5-yl)phenoxy)ethyl) succinate. Orange red solid, yield: 28.3%, m.p. 63–64 °C. ^{1}H NMR ($CDCl_3$, 400 MHz), δ (ppm): 7.63, 7.00 (each 2H, d, $J_A = J_B = 8.6$ Hz, Ar–H), 7.40 (1H, s, 8″-CH), 6.16 (1H, s, 17-CH_2), 6.07 (1H, d, $J = 10.8$ Hz, 6-OH), 5.88 (1H, s, 14-CH), 5.53 (1H, s, 17-CH_2), 4.62 (1H, dd, $J = 11.2$, 5.5 Hz, 1-CH), 4.46 (2H, m, 5′-CH_2), 4.28, 4.18 (each 1H, d, $J_A = J_B = 10.6$ Hz, 20-CH_2), 4.23 (2H, t, $J = 4.6$ Hz, 6′-CH_2), 3.77 (1H, m, 6-CH), 3.14 (1H, d, $J = 9.2$ Hz, 13-CH), 2.65 (2H, m, 2′-CH_2), 2.61 (4H, m, –CH_2), 2.00 (3H, s, –CH_3), 1.13 (6H, s, 18,19-CH_3); ^{13}C NMR ($CDCl_3$, 100 MHz), δ (ppm): 215.42, 206.31, 171.93, 170.86, 169.84, 161.69, 149.44, 134.82, 128.63 (× 2), 124.69, 120.64, 115.58 (× 2), 95.92, 76.07, 75.94, 75.38, 74.19, 66.10, 63.53, 62.78, 61.63, 59.98, 53.79, 41.14, 39.75, 38.15, 33.57, 32.44, 30.24, 29.70, 29.51, 28.78, 25.16, 21.62, 21.53, 18.10; HRMS (ESI) *m*/*z* calcd for $C_{37}H_{42}O_{11}S_3$ $[M - H]^-$ 757.1811, found 757.1839.

4.1.1.8. Compound **11b**.

(1*S*,4a*R*,5*S*,6*S*,6a*R*,9*S*,11a*S*,11b*S*,14*R*)-1-acetoxy-5,6-dihydroxy-4,4-dimethyl-8-methylene-7-oxododecahydro-1*H*-6,11b-(epoxymethano)-6a,9-methanocyclohepta[*a*]naphthalen-14-yl(3-(4-(3-thioxo-3*H*-1,2-dithiol-5-yl)phenoxy)propyl) succinate. Orange red solid, yield: 39.0%, m.p. 66–68 °C. ^{1}H NMR ($CDCl_3$, 400 MHz), δ (ppm): 7.62, 6.98 (each 2H, d, $J_A = J_B = 8.6$ Hz, Ar–H), 7.40 (1H, s, 8″-CH), 6.15 (1H, s, 17-CH_2), 6.08 (1H, d, $J = 10.8$ Hz, 6-OH), 5.88 (1H, s, 14-CH), 5.52 (1H, s, 17-CH_2), 4.62 (1H, dd, $J = 11.2$, 5.4 Hz, 1-CH), 4.28 (3H, m, 20-CH_2, 5′-CH_2), 4.18 (1H, d, $J = 10.6$ Hz, 20-CH_2), 4.10 (2H, t, $J = 6.0$ Hz, 7′-CH_2), 3.78 (1H, m, 6-CH), 3.14 (1H, d, $J = 9.9$ Hz, 13-CH), 2.61 (2H, m, 2′-CH_2), 2.15 (2H, m, 3′-CH_2), 1.99 (3H, s, –CH_3), 1.47 (2H, m, –CH_2), 1.13 (6H, s, 18,19-CH_3); ^{13}C NMR ($CDCl_3$, 100 M Hz), δ (ppm): 215.15, 206.07, 172.96, 171.95, 170.92, 169.83, 162.09, 149.44, 134.67, 128.62 (× 2), 124.32, 120.63, 115.47 (× 2), 95.92, 75.96, 75.37, 74.16, 64.80, 63.53, 61.62, 61.48, 59.98, 53.78, 41.12, 39.75, 38.14, 33.56, 32.43, 30.24, 29.70, 29.54, 28.83, 28.40, 25.16, 21.61, 21.53, 18.08; HRMS (ESI) *m*/*z* calcd for $C_{38}H_{44}O_{11}S_3$ $[M - H]^-$ 771.1968, found 771.1999.

4.1.1.9. Compound **12b**.

(1*S*,4a*R*,5*S*,6*S*,6a*R*,9*S*,11a*S*,11b*S*,14*R*)-1-acetoxy-5,6-dihydroxy-4,4-dimethyl-8-methylene-7-oxododecahydro-1*H*-6,11b-(epoxymethano)-6a,9-methanocyclohepta[*a*]naphthalen-14-yl(6-(4-(3-

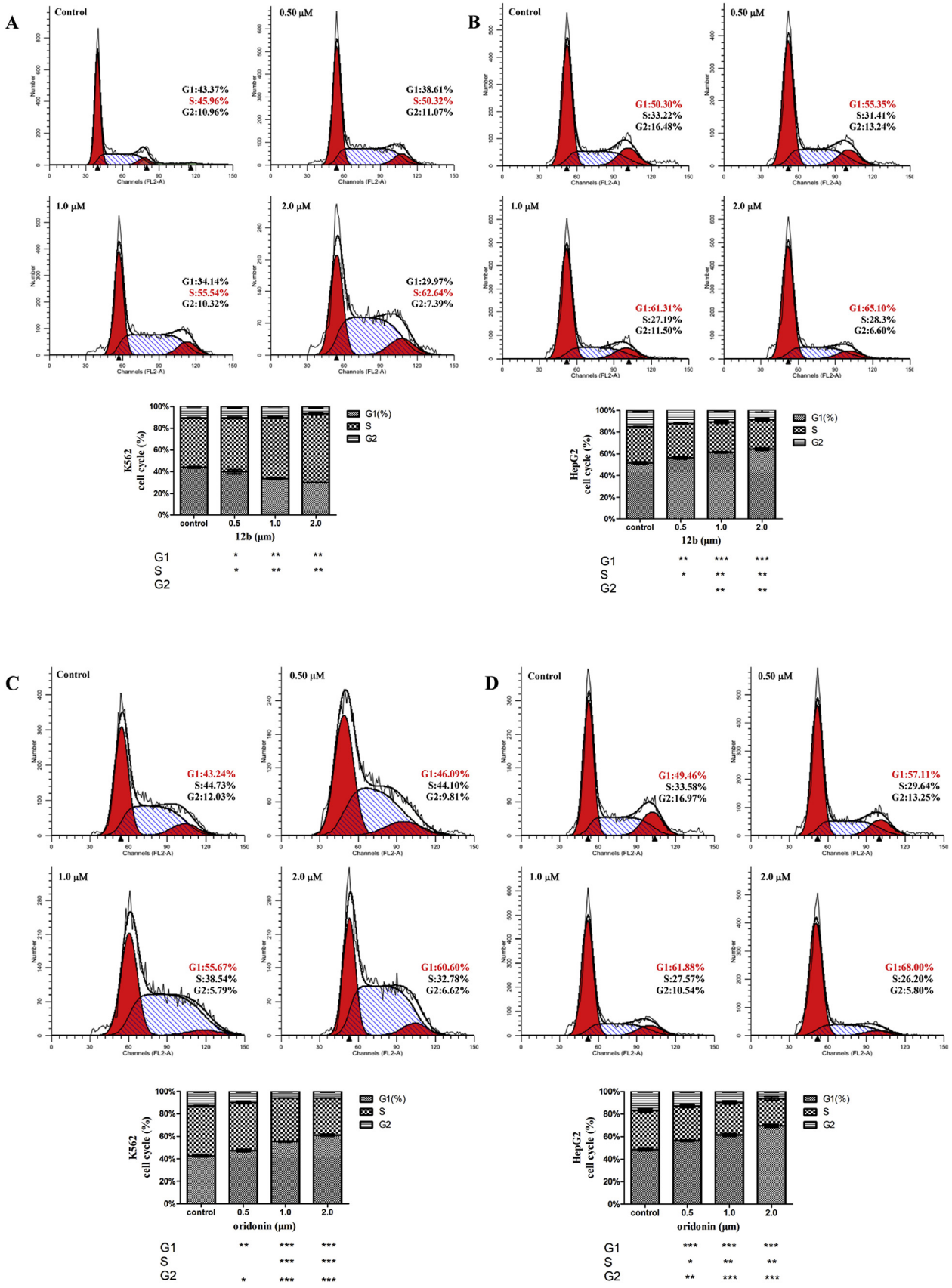

Fig. 4. 12b significantly induced cell cycle arrest. (A) Effect of **12b** on cell cycle distribution of K562 cells. (B) Effect of **12b** on cell cycle distribution of HepG2 cells. (C) Effect of oridonin on cell cycle distribution of K562 cells. (D) Effect of oridonin on cell cycle distribution of HepG2 cells. After the treatment with **12b** or oridonin (0, 0.50, 1.0 and 2.0 μM) for 48 h, K562 or HepG2 cells were stained with PI and cell cycle distribution was investigated by flow cytometer. Data are represented as mean ± SD of three independent experiments. $^{*}p < 0.05$, $^{**}p < 0.01$, and $^{***}p < 0.001$ compared with control group.

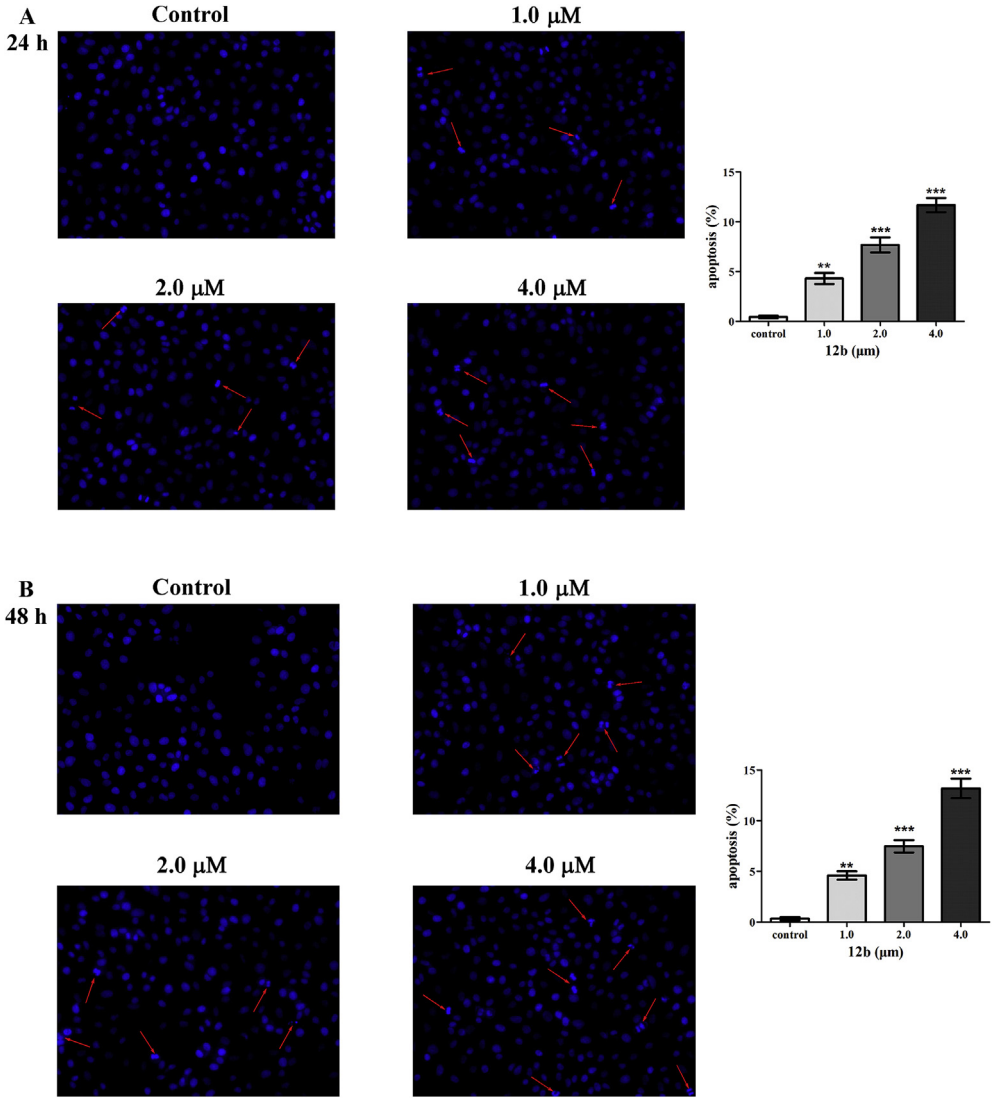

Fig. 5. Effects of **12b** on morphology of K562 cells. (A) Cell morphology after 24 h of **12b** treatment. (B) Cell morphology after 48 h of **12b** treatment. K562 cells were incubated with **12b** (1.0, 2.0 and 4.0 μM) for 24 h and 48 h and then stained with Hoechst 33258 to monitor apoptosis under the fluorescence microscope. The red arrows were pointed to K562 cells with chromatin condensation and fragmentation of cell nuclei. Data are represented as mean ± SD of three independent experiments. $^{*}p < 0.05$, $^{**}p < 0.01$, and $^{***}p < 0.001$ compared with control group. (For interpretation of the references to color in this figure legend, the reader is referred to the Web version of this article.)

thioxo-3*H*-1,2-dithiol-5-yl)phenoxy)hexyl) succinate. Orange red solid, yield: 29.6%, m.p. 71–73 °C. ^{1}H NMR ($CDCl_3$, 400 MHz), δ (ppm): 7.61, 6.96 (each 2H, d, $J_A = J_B = 8.9$ Hz, Ar–H), 7.40 (1H, s, 8″-CH), 6.16 (1H, s, 17-CH_2), 6.09 (1H, d, $J = 10.5$ Hz, 6-OH), 5.88 (1H, s, 14-CH), 5.52 (1H, s, 17-CH_2), 4.62 (1H, dd, $J = 11.2$, 5.4 Hz, 1-CH), 4.28, 4.19 (each 1H, d, $J_A = J_B = 10.6$ Hz, 20-CH_2), 4.09 (2H, m, 5′-CH_2), 4.02 (2H, t, $J = 6.3$ Hz, 10′-CH_2), 3.78 (1H, m, 6-CH), 3.16 (1H, d, $J = 9.9$ Hz, 13-CH), 2.60 (2H, m, 2′-CH_2), 1.99 (3H, s, –CH_3), 1.12 (6H, s, 18,19-CH_3); ^{13}C NMR ($CDCl_3$, 100 MHz), δ (ppm): 215.11, 206.11, 173.13, 172.06, 171.00, 169.84, 162.50, 149.44, 134.57, 128.59 (× 2), 124.01, 120.58, 115.44 (× 2), 95.94, 76.03, 75.38, 74.10, 68.23, 64.83, 63.52, 61.60, 60.04, 53.78, 41.10, 39.75, 38.15, 33.57, 32.42, 30.23, 29.70, 29.59, 28.92, 28.89, 28.46, 25.63, 25.17, 21.60, 21.53, 18.06; HRMS (ESI) *m*/*z* calcd for $C_{41}H_{50}O_{11}S_3$ $[M - H]^-$ 813.2437, found 813.2459.

4.1.1.10. Compound ***13b***.

(1*S*,4a*R*,5*S*,6*S*,6a*R*,9*S*,11a*S*,11b*S*,14*R*)-1-acetoxy-5,6-dihydroxy-4,4-dimethyl-8-methylene-7-oxododecahydro-1*H*-6,11b-(epoxymethano)-6a,9-methanocyclohepta[*a*]naphthalen-14-yl(2-(4-(3-thioxo-3*H*-1,2-dithiol-5-yl)phenoxy)ethyl) glutarate. Orange red solid, yield: 33.6%, m.p. 65–67 °C. ^{1}H NMR ($CDCl_3$, 400 MHz), δ (ppm): 7.63, 7.00 (each 2H, d, $J_A = J_B = 8.6$ Hz, Ar–H), 7.40 (1H, s, 8″-CH), 6.16 (1H, s, 17-CH_2), 6.05 (1H, d, $J = 10.5$ Hz, 6-OH), 5.84 (1H, s, 14-CH), 5.50 (1H, s, 17-CH_2), 4.61 (1H, dd, $J = 11.1$, 5.4 Hz, 1-CH), 4.44 (2H, t, $J = 4.7$ Hz, 6′-CH_2), 4.27, 4.18 (each 1H, d, $J_A = J_B = 10.5$ Hz, 20-CH_2), 4.23 (2H, t, $J = 4.8$ Hz, 7′-CH_2), 4.07 (1H, s, –OH), 3.77 (1H, m, 6-CH), 3.15 (1H, d, $J = 9.2$ Hz, 13-CH), 2.58–2.32 (8H, m, –CH_2), 2.00 (3H, s, –CH_3), 1.13 (3H, s, –CH_3), 1.12 (3H, s, –CH_3); ^{13}C NMR ($CDCl_3$, 100 MHz), δ (ppm): 215.22, 206.06, 172.52, 171.34, 169.86, 161.72, 149.42, 134.83, 128.66 (× 2), 124.69, 120.53, 115.56 (× 2), 96.03, 77.20, 76.06, 75.37, 74.03, 66.15, 63.55, 62.42, 61.56, 60.07, 53.76, 41.12, 39.77, 38.15, 33.57, 33.45, 32.87, 32.40, 30.24, 29.69, 25.17, 21.53, 19.74, 18.04; HRMS (ESI) *m*/*z* calcd for $C_{38}H_{44}O_{11}S_3$ $[M - H]^-$ 771.1968, found 771.2000.

4.1.1.11. Compound ***14b***.

(1*S*,4a*R*,5*S*,6*S*,6a*R*,9*S*,11a*S*,11b*S*,14*R*)-1-acetoxy-5,6-dihydroxy-4,4-

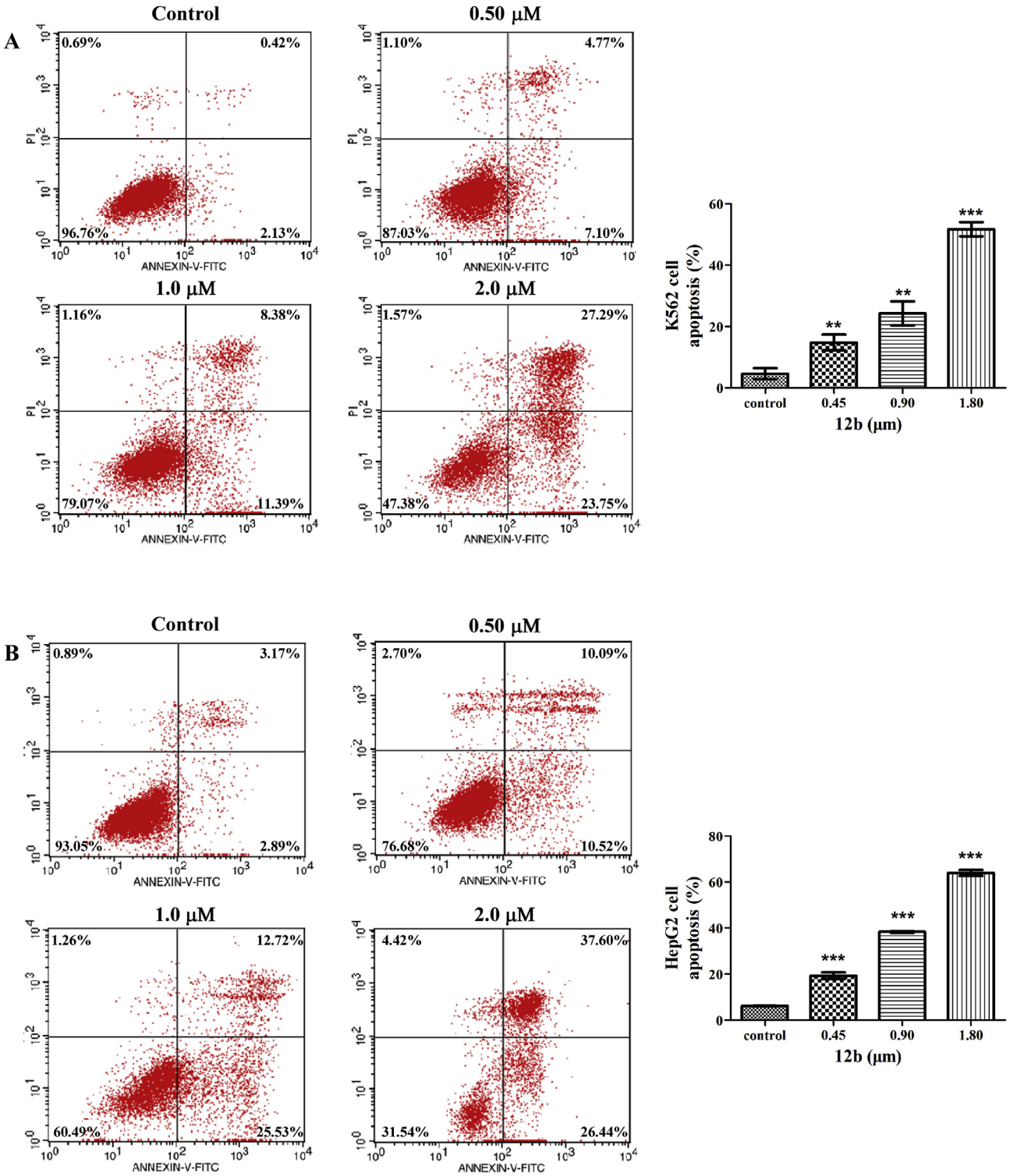

Fig. 6. Effects of **12b** on induction of apoptosis. (A) **12b** induced apoptosis in K562 cells. (B) **12b** induced apoptosis in HepG2 cells. K562 cells were treated with **12b** (0.50, 1.0 and 2.0 μM) for 48 h followed by annexin V/PI staining for 15 min in darkness. Flow cytometric analysis was used to detect apoptosis in K562 cells. Apoptotic cells were on the right panels of each image. Data are represented as mean ± SD of three independent experiments. $^{*}p < 0.05$, $^{**}p < 0.01$, and $^{***}p < 0.001$ compared with control group.

dimethyl-8-methylene-7-oxododecahydro-1*H*-6,11b-(epoxymethano)-6a,9-methanocyclohepta[*a*]naphthalen-14-yl(3-(4-(3-thioxo-3*H*-1,2-dithiol-5-yl)phenoxy)propyl) glutarate. Orange red solid, yield: 41.6%, m.p. 66–68 °C. ^{1}H NMR ($CDCl_3$, 400 MHz), δ (ppm): 7.62, 6.98 (each 2H, d, $J_A = J_B = 8.6$ Hz, Ar–H), 7.40 (1H, s, 8″-CH), 6.15 (1H, s, 17-CH_2), 6.06 (1H, d, $J = 10.5$ Hz, 6-OH), 5.84 (1H, s, 14-CH), 5.51 (1H, s, 17-CH_2), 4.63 (1H, dd, $J = 11.2$, 5.5 Hz, 1-CH), 4.28 (2H, t, $J = 6.3$ Hz, 6′-CH_2), 4.26 (1H, m, 20-CH_2), 4.19 (1H, d, $J = 10.6$ Hz, 20-CH_2), 4.10 (2H, t, $J = 6.1$ Hz, 8′-CH_2), 3.77 (1H, dd, $J = 10.3$, 6.6 Hz, 6-CH), 3.15 (1H, d, $J = 9.2$ Hz, 13-CH), 2.35 (4H, m, $-CH_2$), 2.14, 1.91 (each 2H, m, 2′-CH_2, 4′-CH_2), 2.00 (3H, s, $-CH_3$), 1.12 (6H, s, 18, 19-CH_3); ^{13}C NMR ($CDCl_3$, 100 MHz), δ (ppm): 215.17,

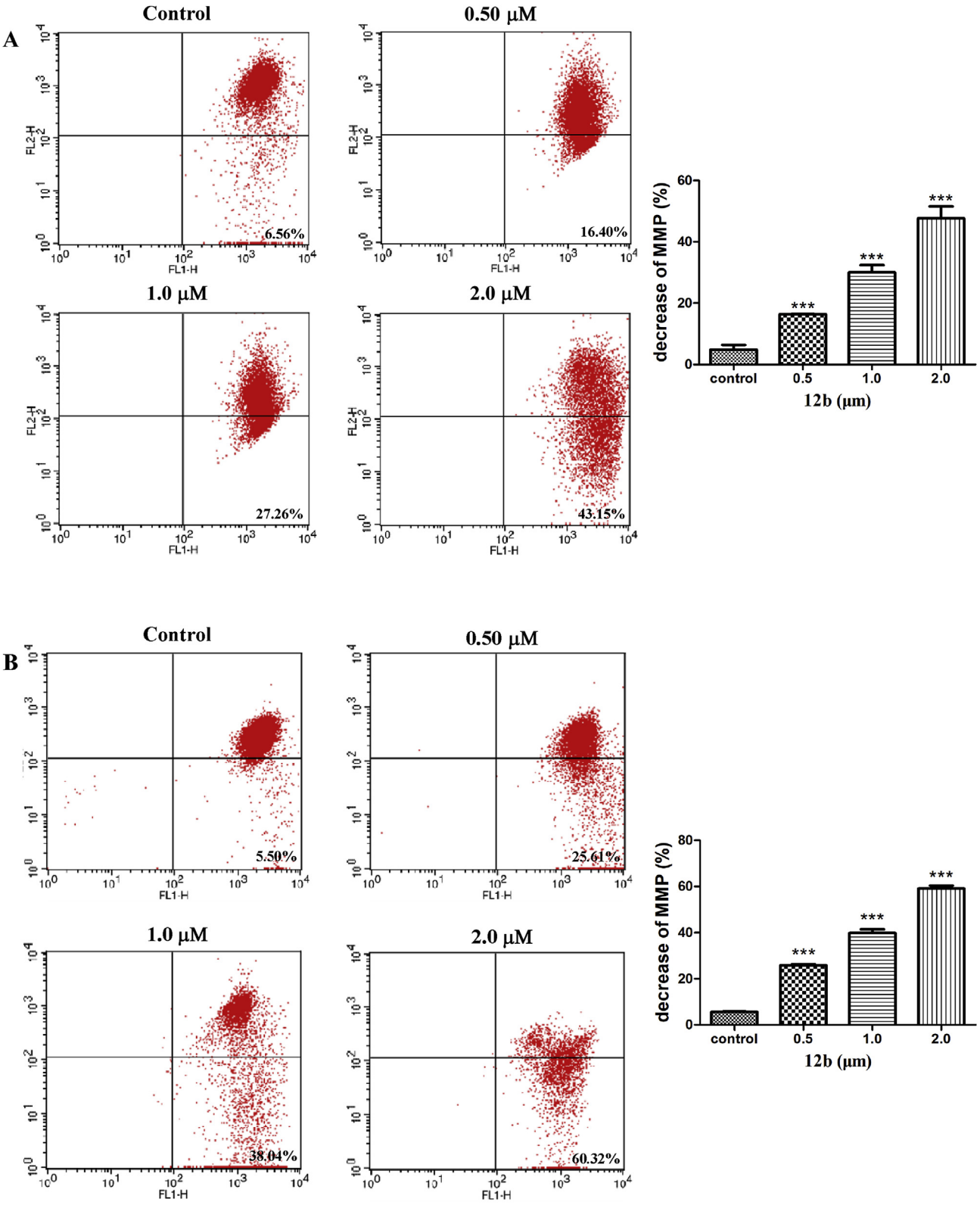

Fig. 7. Decrease of mitochondrial membrane potentials triggered by **12b**. (A) Decrease of mitochondrial membrane potentials in K562 cells. (B) Decrease of mitochondrial membrane potentials in HepG2 cells. After the treatment with **12b** (0.50, 1.0 and 2.0 μM) for 48 h, K562 and HepG2 cells were fixed and labeled with JC-1 for flow cytometry analysis. K562 and HepG2 cells with decreased mitochondrial membrane potentials were on the bottom right panels of each image. Data are represented as mean ± SD of three independent experiments. $^{*}p < 0.05$, $^{**}p < 0.01$, and $^{***}p < 0.001$ compared with control group.

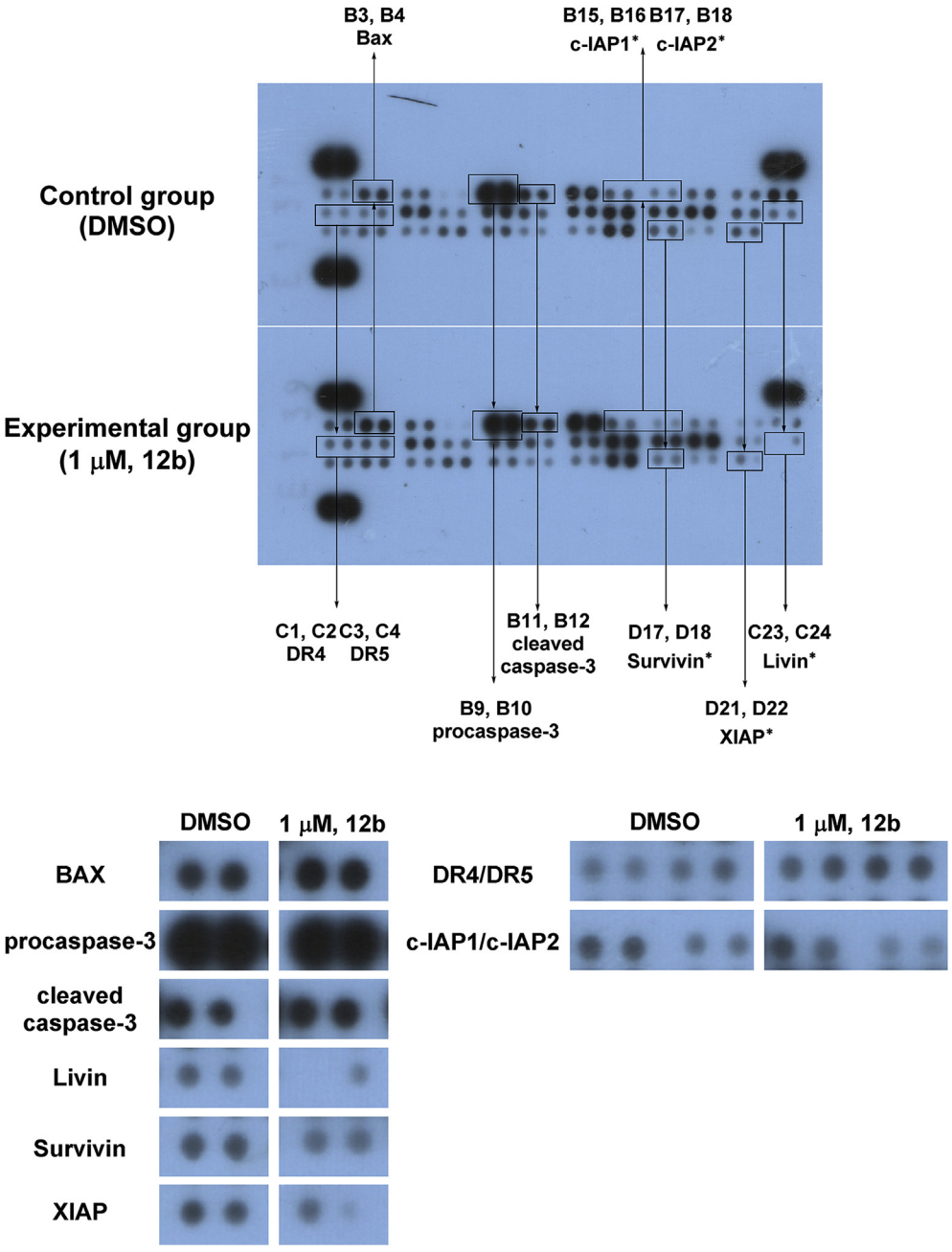

Fig. 8. Effects of **12b** on apoptosis-related protein expression of K562 cells. The total cell lysates were collected from K562 cells pretreated with 1 μM **12b** for 24 h and then seeded in Human Apoptosis Array kit. Anti-apoptotic proteins were labeled with "*". Some dots of changed apoptosis-related proteins were locally amplified.

206.07, 172.98, 172.59, 171.34, 169.84, 162.10, 149.42, 134.69, 128.63 (× 2), 124.32, 120.53, 115.47 (× 2), 96.03, 76.08, 75.36, 74.02, 64.79, 63.56, 61.56, 61.08, 60.07, 53.76, 41.12, 39.77, 38.14, 33.56, 32.99, 32.41, 30.24, 29.69, 28.45, 25.17, 21.58, 21.53, 19.78, 18.04; HRMS (ESI) *m/z* calcd for $C_{39}H_{46}O_{11}S_3$ $[M-H]^-$ 785.2124, found 785.2172.

*4.1.1.12. Compound **15b**.*

(1*S*,4a*R*,5*S*,6*S*,6a*R*,9*S*,11a*S*,11b*S*,14*R*)-1-acetoxy-5,6-dihydroxy-4,4-dimethyl-8-methylene-7-oxododecahydro-1*H*-6,11b-(epoxymethano)-6a,9-methanocyclohepta[*a*]naphthalen-14-yl(6-(4-(3-thioxo-3*H*-1,2-dithiol-5-yl)phenoxy)hexyl) glutarate. Orange red solid, yield: 33.4%, m.p. 72–74 °C. ^{1}H NMR ($CDCl_3$, 400 MHz), δ (ppm): 7.61, 6.96 (each 2H, d, $J_A = J_B = 8.6$ Hz, Ar–H), 7.40 (1H, s, 8″-CH), 6.15 (1H, s, 17-CH_2), 6.10 (1H, d, $J = 10.5$ Hz, 6-OH), 5.84 (1H, s, 14-CH), 5.51 (1H, s, 17-CH_2), 4.63 (1H, dd, $J = 11.2$, 5.5 Hz, 1-CH), 4.28, 4.18 (each 1H, d, $J_A = J_B = 10.6$ Hz, 20-CH_2), 4.07 (2H, t, $J = 6.7$ Hz, 6′-CH_2), 4.02 (2H, t, $J = 6.4$ Hz, 11′-CH_2), 3.78 (1H, dd, $J = 10.2$, 6.6 Hz, 6-CH), 3.16 (1H, d, $J = 9.9$ Hz, 13-CH), 2.39–2.30 (4H, m, $-CH_2$), 2.00 (3H, s, $-CH_3$), 1.91 (2H, m, 2′-CH_2), 1.83 (2H, m, 4′-CH_2), 1.13 (6H, s, 18, 19-CH_3); ^{13}C NMR ($CDCl_3$, 100 M Hz), δ (ppm): 215.27, 206.13, 173.12, 172.73, 171.43, 169.85, 162.51, 149.43, 134.58, 128.58 (× 2), 124.01, 120.49, 115.45 (× 2), 96.03, 76.10, 75.37, 73.97, 68.24, 64.44, 63.54, 61.56, 60.12, 53.75, 41.12, 39.77, 38.15, 33.57 (× 2), 33.07, 32.39, 30.23, 29.69 (× 2), 28.92, 28.51, 25.64 (× 2), 25.17, 21.56, 19.84, 18.03; HRMS (ESI) *m/z* calcd for $C_{42}H_{52}O_{11}S_3$ $[M-H]^-$ 827.2594, found 827.2588.

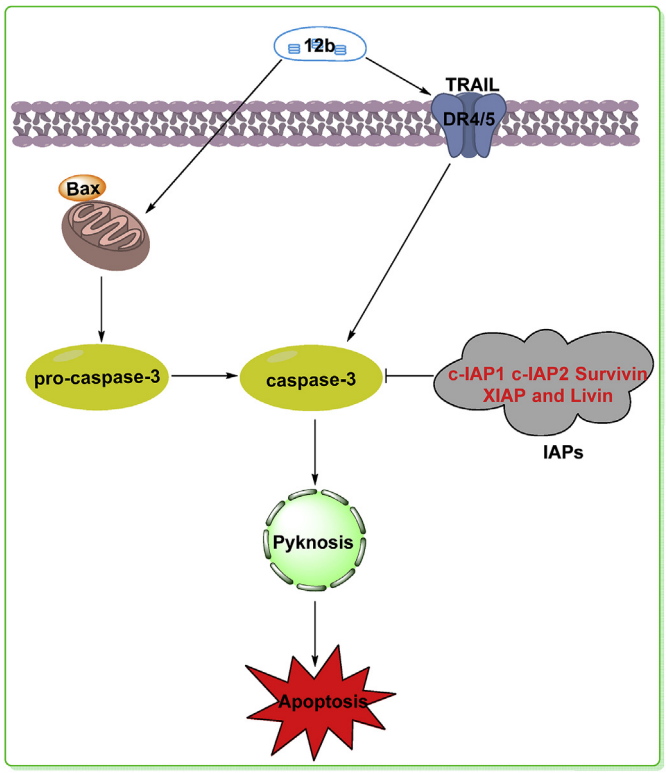

Fig. 9. The apoptosis-related pathways would involve in **12b** treated K562 cells.

4.1.1.13. Compound ***10c***.

2-(4-(3-thioxo-3*H*-1,2-dithiol-5-yl)phenoxy)ethyl((1-*S*,4a*R*,5*S*,6*S*,6a*R*,9*S*,11a*S*,11b*S*,14*R*)-1,5,6-trihydroxy-4,4-dimethyl-8-methylene-7-oxododecahydro-1*H*-6,11b-(epoxymethano)-6a,9-methanocyclohepta[*a*]naphthalen-14-yl) succinate. Orange red solid, yield: 27.4%, m.p. 68–70 °C. ^{1}H NMR ($CDCl_3$, 400 MHz), δ (ppm): 7.63, 7.01 (each 2H, d, $J_A = J_B = 8.6$ Hz, Ar–H), 7.40 (1H, s, 8″-H), 6.15 (1H, s, 17-CH_2), 6.05 (1H, d, $J = 10.7$ Hz, 6-OH), 5.89 (1H, s, 17-CH_2), 5.51 (1H, s, 14-CH), 4.46 (2H, m, 5′-CH_2), 4.29, 4.06 (each 1H, d, $J = 10.5$ Hz, 20-CH_2), 4.24 (2H, t, $J = 4.6$ Hz, 6′-CH_2), 3.75 (1H, d, 10.0 Hz, 6-CH), 3.49 (1H, dd, $J = 11.1$, 5.7 Hz, 1-CH), 3.14 (1H, d, $J = 9.8$ Hz, 13-CH), 2.65 (2H, m, 3′-CH_2), 2.59 (2H, m, 2′-CH_2), 2.54–2.41 (2H, m, –CH_2), 2.22, 1.97 (each 1H, m, –CH_2), 1.93 (2H, m, –CH_2), 1.80–1.52 (2H, m, –CH_2), 1.46 (2H, m, –CH_2), 1.11 (3H, s, 18-CH_3), 1.10 (3H, s, 19-CH_3); ^{13}C NMR ($CDCl_3$, 100 M Hz), δ (ppm): 215.20, 206.36, 172.85, 171.96, 170.76, 161.77, 149.90, 134.82, 128.63 (× 2), 124.64, 120.28, 115.64 (× 2), 96.05, 76.18, 74.33, 73.49, 66.15, 63.37, 62.73, 61.93, 59.49, 54.68, 41.33, 38.65, 33.73, 32.61, 30.53, 30.06, 29.69, 29.53, 28.83, 21.75, 19.89; HRMS (ESI) *m*/*z* calcd for $C_{35}H_{40}O_{10}S_3$ [M – H]$^-$ 715.1706, found 715.1731.

4.1.1.14. Compound ***11c***.

3-(4-(3-thioxo-3*H*-1,2-dithiol-5-yl)phenoxy)propyl((1*S*,4a*R*,5*S*,6*S*,6a*R*,9*S*,11a*S*,11b*S*,14*R*)-1,5,6-trihydroxy-4,4-dimethyl-8-methylene-7-oxododecahydro-1*H*-6,11b-(epoxymethano)-6a,9-methanocyclohepta[*a*]naphthalen-14-yl) succinate. Orange red solid, yield: 32.6%, m.p. 71–73 °C. ^{1}H NMR ($CDCl_3$, 400 MHz), δ (ppm): 7.63, 7.00 (each 2H, d, $J_A = J_B = 8.0$ Hz, Ar–H), 7.42 (1H, s, 8″-H), 6.14 (1H, s, 17-CH_2), 6.06 (1H, d, $J = 8.5$ Hz, 6-OH), 5.90 (1H, s, 17-CH_2), 5.51 (1H, s, 14-CH), 4.30 (3H, m, 5′-CH_2, 20-CH_2), 4.10 (3H, m, 7′-CH_2, 20-CH_2), 3.75 (1H, m, 6-CH), 3.50 (1H, dd, $J = 11.1$, 5.5 Hz, 1-CH), 3.12 (1H, d, $J = 9.7$ Hz, 13-CH), 2.58 (4H, m, –CH_2), 2.16 (2H, t, $J = 5.8$ Hz, 2′-CH_2), 1.96, 1.76 (each 1H, m, –CH_2), 1.70–1.43 (6H, m, –CH_2), 1.11 (6H, s, 18-CH_3, 19-CH_3); ^{13}C NMR ($CDCl_3$, 100 M Hz), δ (ppm): 215.12, 206.37, 173.16, 172.04, 170.90, 162.23, 149.87, 134.63, 128.61 (× 2), 124.21, 120.27, 115.55 (× 2), 96.05, 76.12, 74.32, 73.43, 64.87, 63.42, 61.94, 61.31, 59.51, 54.67, 41.34, 41.30, 38.63, 33.73, 32.61, 30.51, 30.06, 29.54, 28.86, 28.49, 21.75, 19.93; HRMS (ESI) *m*/*z* calcd for $C_{36}H_{42}O_{10}S_3$ [M – H]$^-$ 729.1862, found 729.1890.

4.1.1.15. Compound ***12c***.

6-(4-(3-thioxo-3*H*-1,2-dithiol-5-yl)phenoxy)hexyl((1*S*,4a*R*,5*S*,6*S*,6a*R*,9*S*,11a*S*,11b*S*,14*R*)-1,5,6-trihydroxy-4,4-dimethyl-8-methylene-7-oxododecahydro-1*H*-6,11b-(epoxymethano)-6a,9-methanocyclohepta[*a*]naphthalen-14-yl) succinate. Orange red solid, yield: 40.2%, m.p. 64–66 °C. ^{1}H NMR ($CDCl_3$, 400 MHz), δ (ppm): 7.61, 6.97 (each 2H, d, $J_A = J_B = 8.7$ Hz, Ar–H), 7.40 (1H, s, 8″-H), 6.15 (2H, s, 17-CH_2), 6.09 (2H, d, $J = 10.2$ Hz, 6-OH), 5.91 (2H, s, 17-CH_2), 5.52 (2H, s, 14-CH), 4.30 (2H, d, $J = 10.2$ Hz, 20-CH_2), 4.08 (6H, m, 20-CH_2, 5′-CH_2), 4.03, 3.41 (each 2H, t, $J = 6.6$ Hz, 10′-CH_2), 3.76 (2H, m, 6-CH), 3.50 (2H, dd, $J = 11.2$, 5.7 Hz, 1-CH), 3.16 (2H, d, $J = 9.7$ Hz, 13-CH), 2.58 (8H, m, –CH_2), 1.99–1.71 (10H, m, –CH_2), 1.70–1.41 (18H, m, –CH_2), 1.12 (12H, s, 18-CH_3, 19-CH_3); ^{13}C NMR ($CDCl_3$, 100 M Hz), δ (ppm): 215.17, 206.41, 173.15, 172.10, 170.93, 162.64, 149.90, 134.57, 128.60 (× 2), 120.24, 115.48 (× 2), 96.08, 76.24, 74.24, 73.52, 68.25, 64.76, 63.35, 61.91, 59.55, 54.67, 41.34, 38.67, 33.73, 32.59, 30.51, 30.07, 29.69, 29.57, 28.90, 28.44, 28.37, 27.77, 25.62, 25.09, 21.72, 19.87; HRMS (ESI) *m*/*z* calcd for $C_{69}H_{90}O_{19}S_3$ [M+H]$^+$ 1319.5316, found 1319.5395.

4.1.1.16. Compound ***13c***.

2-(4-(3-thioxo-3*H*-1,2-dithiol-5-yl)phenoxy)ethyl((1-*S*,4a*R*,5*S*,6*S*,6a*R*,9*S*,11a*S*,11b*S*,14*R*)-1,5,6-trihydroxy-4,4-dimethyl-8-methylene-7-oxododecahydro-1*H*-6,11b-(epoxymethano)-6a,9-methanocyclohepta[*a*]naphthalen-14-yl) glutarate. Orange red solid, yield: 31.8%, m.p. 70–72 °C. ^{1}H NMR ($CDCl_3$, 400 MHz), δ (ppm): 7.63, 6.99 (each 2H, d, $J_A = J_B = 8.8$ Hz, Ar–H), 7.40 (1H, s, 8″-H), 6.13 (1H, s, 17-CH_2), 6.05 (1H, d, $J = 8.6$ Hz, 6-OH), 5.87 (1H, s, 17-CH_2), 5.50 (1H, s, 14-CH), 4.30, 4.07 (each 1H, d, $J = 10.4$ Hz, 20-CH_2), 4.44, 4.23 (each 2H, t, $J = 4.4$ Hz, 6′-CH_2, 7′-CH_2), 3.74 (1H, m, 6-CH), 3.50 (1H, dd, $J = 11.2$, 5.7 Hz, 1-CH), 3.15 (1H, d, $J = 9.8$ Hz, 13-CH), 2.60, 2.24 (each 1H, m, 3′-CH_2), 2.42–2.33 (4H, m, 2′-CH_2, 4′-CH_2), 1.94 (4H, m, –CH_2), 1.11 (3H, s, 18-CH_3), 1.10 (3H, s, 19-CH_3); ^{13}C NMR ($CDCl_3$, 100 M Hz), δ (ppm): 215.19, 206.38, 172.88, 172.57, 171.27, 161.75, 149.86, 134.80, 128.66 (× 2), 124.63, 120.19, 115.58 (× 2), 96.15, 76.33, 74.16, 73.48, 66.15, 63.41, 62.38, 61.88, 59.60, 54.62, 41.34, 41.31, 38.64, 33.73, 33.44, 32.89, 32.58, 30.52, 30.07, 29.69, 21.70, 19.83; HRMS (ESI) *m*/*z* calcd for $C_{36}H_{42}O_{10}S_3$ [M – H]$^-$ 729.1862, found 729.1889.

4.1.1.17. Compound ***14c***.

3-(4-(3-thioxo-3*H*-1,2-dithiol-5-yl)phenoxy)propyl((1*S*,4a*R*,5*S*,6*S*,6a*R*,9*S*,11a*S*,11b*S*,14*R*)-1,5,6-trihydroxy-4,4-dimethyl-8-methylene-7-oxododecahydro-1*H*-6,11b-(epoxymethano)-6a,9-methanocyclohepta[*a*]naphthalen-14-yl) glutarate. Orange red solid, yield: 30.2%, m.p. 74–75 °C. ^{1}H NMR ($CDCl_3$, 400 MHz), δ (ppm): 7.62, 6.98 (each 2H, d, $J_A = J_B = 8.7$ Hz, Ar–H), 7.40 (1H, s, 8″-H), 6.13 (1H, s, 17-CH_2), 6.05 (1H, s, 6-OH), 5.87 (1H, s, 17-CH_2), 5.50 (1H, s, 14-CH), 4.30, 4.07 (each 1H, d, $J = 10.8$ Hz, 20-CH_2), 4.27, 4.10 (each 2H, t, $J = 6.4$ Hz, –CH_2), 3.75 (1H, brs, 6-CH), 3.50 (1H, dd, $J = 11.1$, 5.7 Hz, 1-CH), 3.15 (1H, d, $J = 9.8$ Hz, 13-CH), 2.60, 2.25 (each 1H, m, 3′-CH_2), 2.34 (4H, m, -2′-CH_2, 4′-CH_2), 2.15, 1.90 (each 2H, m, –CH_2), 1.80–1.42 (8H, m, –CH_2), 1.12 (3H, s, 18-CH_3), 1.11 (3H, s, 19-CH_3); ^{13}C NMR ($CDCl_3$, 100 M Hz), δ (ppm): 215.13, 206.38, 173.10, 172.63, 171.28, 162.15, 149.86, 134.66, 128.64 (× 2), 124.27, 120.18, 115.49 (× 2), 96.17, 76.34, 74.15, 73.47, 64.82,

63.42, 61.88, 61.06, 59.61, 54.62, 41.34, 41.32, 38.64, 33.74, 33.53, 33.03, 32.58, 30.52, 30.07, 29.70, 28.44, 21.71, 19.84; HRMS (ESI) *m*/*z* calcd for $C_{37}H_{44}O_{10}S_3$ $[M-H]^-$ 743.2019, found 743.2034.

*4.1.1.18. Compound **15c**.*
6-(4-(3-thioxo-3*H*-1,2-dithiol-5-yl)phenoxy)hexyl((1*S*,4a*R*,5*S*,6*S*,6a*R*,9*S*,11a*S*,11b*S*,14*R*)-1,5,6-trihydroxy-4,4-dimethyl-8-methylene-7-oxododecahydro-1*H*-6,11b-(epoxymethano)-6a,9-methanocyclohepta[*a*]naphthalen-14-yl) glutarate. Orange red solid, yield: 37.1%, m.p. 67–69 °C. ^{1}H NMR ($CDCl_3$, 400 MHz), δ (ppm): 7.61, 6.97 (each 2H, d, $J_A = J_B = 8.8$ Hz, Ar–H), 7.40 (1H, s, 8″-H), 6.14 (2H, s, 17-CH_2), 6.06 (2H, d, $J = 10.2$ Hz, 6-OH), 5.87 (2H, s, 17-CH_2), 5.50 (2H, s, 14-CH), 4.30 (2H, d, $J = 10.2$ Hz, 20-CH_2), 4.10–4.01 (8H, m, 20-CH_2, 5′-CH_2, 10′-CH_2), 3.76 (2H, t, $J = 7.4$ Hz, 6-CH), 3.50 (2H, dd, $J = 11.1$, 5.6 Hz, 1-CH), 3.41 (2H, t, $J = 6.7$ Hz, 10′-CH_2), 3.17 (2H, d, $J = 9.9$ Hz, 13-CH), 2.60, 2.24 (each 2H, m, 3′-CH_2), 2.33 (8H, m, 2′-CH_2, 4′-CH_2), 1.90 (4H, t, $J = 7.3$ Hz, $-CH_2$), 1.83 (4H, m, $-CH_2$), 1.69–1.60 (8H, m, $-CH_2$), 1.53–1.43 (8H, m, $-CH_2$), 1.12 (12H, s, 18-CH_3, 19-CH_3); ^{13}C NMR ($CDCl_3$, 100 M Hz), δ (ppm): 215.10, 206.42, 173.23, 172.78, 171.35, 162.55, 149.87, 134.54, 128.60 (× 2), 123.97, 120.14, 115.48 (× 2), 96.17, 76.40, 74.12, 73.47, 68.25, 64.43, 63.40, 61.87, 59.66, 54.62, 41.34, 38.65, 33.73, 33.56, 33.10, 32.57, 30.51, 30.06, 28.92, 28.50, 27.77, 25.63, 25.13, 21.69, 19.82; HRMS (ESI) *m*/*z* calcd for $C_{71}H_{94}O_{19}S_3$ $[M+H]^+$ 1347.5629, found 1347.5678.

4.2. MTT assay and trypan blue assay

MTT assay and trypan blue assay were carried out to investigate the cytotoxicity of all derivatives against five cancer cell lines and two normal cells. All cells were seeded in standard 96-well plates under the condition of humidified 5% CO_2 and kept at 37 °C to simulate human body temperature. After 24 h, gradient diluted target derivatives (DMSO in each well <0.5%) were added and incubated for 72 h. MTT solution (0.5 mg/mL) was added to each well and cultivated for another 4 h, and then removed the media followed by dissolution formazan crystals in DMSO (200 μL). Finally, the absorbance (OD) of each well was determined quantitatively by Microplate Reader at 490 nm wavelength and half inhibition rates (IC_{50}) were calculated by a data analysis software. In trypan blue assay, after 72 h incubated with all derivatives, cells were stained with 0.4% trypan blue for 3 min and then observed by using optical microscopy.

4.3. H_2S release experiment

Na_2S was dissolved in sodium phosphate buffer (20 mM, pH 7.4) in 100 mL volumetric flask, which was used as the stock solution and then standard solutions of 5, 10, 20, 40, 60, 80, 100 and 150 μM in 50 mL volumetric flask were prepared. 1 mL of each standard solution was added into methylene blue (MB^+) cocktail: 200 μL of 30 mM $FeCl_3$ in 1.2 M HCl, 200 μL of 20 mM N,*N*-dimethyl-1,4-phenylenediamine sulfate in 7.2 M HCl and 100 μL of 1% w/v $Zn(OAc)_2$ in H_2O and stored for 20 min at room temperature (each reaction was carried out in triplicate). Later, each of colorimetric cuvette was placed in UV–Vis spectrophotometer at 670 nm to draft the Na_2S calibration curve [62]. Target derivatives were added into the mixture of THF and PBS in the presence of 1 mM TCEP (an effective mercaptan reductant) which was used as an accelerator. At different time points, the mixture (2 mL) was transferred to colorimetric cuvette included methylene blue (MB^+) cocktail. Ultimately, each of colorimetric cuvette was placed in UV–Vis spectrophotometer at 670 nm after 20 min at room temperature. According to the absorbance of each compound, the H_2S release was calculated through standard curve.

4.4. Cell cycle analysis

K562 and HepG2 cells were seeded in 6-well plates and incubated with **12b** or oridonin for 48 h and then harvested by centrifugation. The cells were washed with cold PBS and fixed with 70% ethanol at −20 °C overnight. After re-centrifugation, all cells were suspended again using PBS buffer and then incubated with RNase A (1 mg/mL) and PI (0.1 mg/mL) for 30 min in darkness. All samples were then analyzed by flow cytometer to determine the distribution of DNA content [63].

4.5. Hoechst 333258 staining

K562 cells were grown on 6-well plates which contained 2 mL medium and adhered for 24 h or 48 h. Later, **12b** (0, 1.0, 2.0 and 4.0 μM) was added into each well and cultured for another 48 h. After mild trypsinization and centrifugation, cells were harvested and washed twice with PBS buffer. Then, using Hoechst mixture (0.5 mg/mL) in PBS buffer to stain cells for 30 min in darkness. After washed by PBS, cells were mounted on slides and analyzed through a DAPI filtered fluorescence microscope.

4.6. Cell apoptosis assay

To uncovered the influence of **12b** on apoptosis, K562 and HepG2 cells were incubated in 6-well plates for 72 h and then different concentrations (0, 0.50, 1.0 and 2.0 μM) of **12b** were injected for another 48 h. After washed twice with PBS, cells were suspended in annexin V binding buffer. Then AV-FITC and PI were added to the mixture at room temperature and incubated for 15 min in darkness. Finally, double-staining cells were measured via flow cytometry to detect apoptotic process.

4.7. Mitochondrial membrane potential assay

K562 and HepG2 cells were grown on 6-well plates and incubated with **12 b** at 0, 0.50, 1.0 and 2.0 μM concentrations for 48 h. After trypsinization, cells were collected and then stained with JC-1 (0.5 mg/mL) at 37 °C in darkness. Washed out excess dye with PBS after 30 min incubation, and then monitored the mitochondrial membrane potentials by flow cytometry.

4.8. Human apoptosis protein array

According to the manufacturer instructions, the relative expression levels of 35 apoptosis-related proteins were investigated after the treatment with **12b** (1 μM) [64]. Diluted cellular extracts were seeded in Human Apoptosis Array kit for 24 h. Washed to remove unbound proteins, and then incubated with a biotinylated detection antibody for 1 h. After that, chemiluminescent signals were detected by digital imaging system.

4.9. Statistical analysis

All data were expressed as the means ± standard deviation (SD), from at least three independent experiments. Statistical analysis and figures were performed by GraphPad.Prism. v5.0.

Declaration of competing interest

The authors declare that they have no known competing financial interests or personal relationships that could have appeared to influence the work reported in this paper.

Acknowledgment

This paper was financially supported by the National Natural Science Foundation of China (21772124, 21502121), Natural Science Foundation of Liaoning Province (20170540858), General Scientific Research Projects of Department of Education in Liaoning Province (2017LQN05), Key Laboratory of Quality Control of TCM of Liaoning Province (17-137-1-00) and Career Development Support Plan for Young and Middle-aged Teachers in Shenyang Pharmaceutical University.

Appendix A. Supplementary data

Supplementary data to this article can be found online at https://doi.org/10.1016/j.ejmech.2019.111978.

References

[1] J. Wu, B. Wu, C. Tang, J. Zhao, Analytical techniques and pharmacokinetics of gastrodia elata blume and its constituents, Molecules 22 (2017) 1137.
[2] C. Tang, J. Wang, J. Yu, L. Wang, M. Cheng, W. Cui, J. Zhao, H. Xiao, Identification, characterization and in vitro neuroprotection of N_6-(4-hydroxybenzyl) adenine riboside and its metabolites, Phytochem. Lett. 20 (2017) 146–150.
[3] Z. Zhang, Y. Tang, B. Yu, J. Ying, B. Wu, J. Wu, J. Zhao, Z. Chen, J. Xu, C. Tang, Chemical composition database establishment and metabolite profiling analysis of Yangyin qingfei decoction, Biomed. Chromatogr. 33 (2019), e4581.
[4] C. Tang, B. Wu, J. Wu, Z. Zhang, B. Yu, Novel strategies using total gastrodin and gastrodigenin, or total gastrodigenin for quality control of *gastrodia elata*, Molecules 23 (2018) 270.
[5] T. Rodrigues, D. Reker, P. Schneider, G. Schneider, Counting on natural products for drug design, Nat. Chem. 8 (2016) 531–541.
[6] D.J. Newman, G.M. Cragg, Natural products as sources of new drugs from 1981 to 2014, J. Nat. Prod. 79 (2016) 629–661.
[7] Y. Tang, Z. Li, L. Lazar, Z. Fang, C. Tang, J. Zhao, Metabolomics workflow for lung cancer: discovery of biomarkers, Clin. Chim. Acta 495 (2019) 436–445.
[8] K. Osawa, H. Yasuda, T. Maruyama, H. Morita, K. Takeya, H. Itokawa, K. Okuda, An investigation of diterpenes from the leaves of *Rabdosia trichocarpa* and their antibacterial activity against oral microorganisms, Chem. Pharm. Bull. 42 (1994) 922–925.
[9] S.S. Hong, S.A. Lee, X.H. Han, J.S. Hwang, C. Lee, D. Lee, J.T. Hong, Y. Kim, H. Lee, B.Y. Hwang, *ent*-Kaurane diterpenoids from *Isodon japonicus*, J. Nat. Prod. 71 (2008) 1055–1058.
[10] S. Aquila, Z.Y. Weng, Y.Q. Zeng, H.D. Sun, J.L. Rios, Inhibition of NF-κB activation and iNOS induction by *ent-kaurane* diterpenoids in LPS-stimulated RAW264.7 murine macrophages, J. Nat. Prod. 72 (2009) 1269–1272.
[11] X. Luo, J.X. Pu, W.L. Xiao, Y. Zhao, X.M. Gao, X.N. Li, H.B. Zhang, Y.Y. Wang, Y. Li, H.D. Sun, Cytotoxic *ent*-kaurane diterpenoids from *Isodon rubescens* var. *lushiensis*, J. Nat. Prod. 73 (2010) 1112–1116.
[12] H.B. Zhang, J.X. Pu, Y.Y. Wang, F. He, Y. Zhao, X.N. Li, X. Luo, W.L. Xiao, Y. Li, H.D. Sun, Four new *ent*-kauranoids from *Isodon rubescens* var. *lushanensis* and data reassignment of dayecrystal B, Chem. Pharm. Bull. 58 (2010) 56–60.
[13] W. Zhao, J.X. Pu, X. Du, J. Su, X.N. Li, J.H. Yang, Y.B. Xue, Y. Li, W.L. Xiao, H.D. Sun, Structure and cytotoxicity of diterpenoids from *Isodon adenolomus*, J. Nat. Prod. 74 (2011) 1213–1220.
[14] R. Zhan, X.N. Li, X. Du, W.G. Wang, K. Dong, J. Su, Y. Li, J.X. Pu, H.D. Sun, Bioactive *ent*-kaurane diterpenoids from *Isodon rosthornii*, J. Nat. Prod. 76 (2013) 1267–1277.
[15] T. Matsumoto, S. Nakamura, N. Kojima, T. Hasei, M. Yamashita, T. Watanabe, H. Matsuda, Antimutagenic activity of *ent*-kaurane diterpenoids from the aerial parts of *Isodon japonicus*, Tetrahedron Lett. 58 (2017) 3574–3578.
[16] H.D. Sun, S.X. Huang, Q.B. Han, Diterpenoids from *Isodon* species and their biological activities, Nat. Prod. Rep. 23 (2006) 673–698.
[17] M. Liu, W.G. Wang, H.D. Sun, J.X. Pu, Diterpenoids from *Isodon* species: an update, Nat. Prod. Rep. 34 (2017) 1090–1140.
[18] E. Fujita, T. Fujita, H. Katayama, M. Shibuya, T. Shingu, Terpenoids. Part XV. Structure and absolute configuration oridonin isolated from *Isodon japonicus* and *Isodon trichocarpus*, J. Chem. Soc. C 21 (1970) 1674–1681.
[19] G.B. Zhou, H. Kang, L. Wang, L. Gao, P. Liu, J. Xie, F.X. Zhang, X.Q. Weng, Z.X. Shen, J. Chen, L.J. Gu, M. Yan, D.E. Zhang, S.J. Chen, Z.Y. Wang, Z. Chen, Oridonin, a diterpenoid extracted from medicinal herbs, targets AML1-ETO fusion protein and shows potent antitumor activity with low adverse effects on t(8;21) leukemia in vitro and in vivo, Blood 109 (2007) 3441–3450.
[20] X. Qi, D. Zhang, X. Xu, F. Feng, G. Ren, Q. Chu, Q. Zhang, K. Tian, Oridonin nanosuspension was more effective than free oridonin on G_2/M cell cycle arrest and apoptosis in the human pancreatic cancer PANC-1 cell line, Int. J. Nanomed. 7 (2012) 1793–1804.
[21] Y. Lu, Y. Sun, J. Zhu, L. Yu, X. Jiang, J. Zhang, X. Dong, B. Ma, Q. Zhang, Oridonin exerts anticancer effect on osteosarcoma by activating PPAR-γ and inhibiting Nrf2 pathway, Cell Death Dis. 9 (2018) 15.
[22] Z. Yao, F. Xie, M. Li, Z. Liang, W. Xu, J. Yang, C. Liu, H. Li, H. Zhou, L.H. Qu, Oridonin induces autophagy via inhibition of glucose metabolism in p53-mutated colorectal cancer cells, Cell Death Dis. 8 (2017) 2633.
[23] J. Zhou, E.J. Yun, W. Chen, Y. Ding, K. Wu, B. Wang, C. Ding, E. Hernandez, J. Santoyo, R.C. Pong, H. Chen, D. He, J. Zhou, J.T. Hsieh, Targeting 3-phosphoinositide-dependent protein kinase 1 associated with drug-resistant renal cell carcinoma using new oridonin analogs, Cell Death Dis. 8 (2017), e2701.
[24] K. Qing, Z. Jin, W. Fu, W. Wang, Z. Liu, X. Li, Z. Xu, J. Li, Synergistic effect of oridonin and a PI3K/mTOR inhibitor on the non-germinal center B cell-like subtype of diffuse large B cell lymphoma, J. Hematol. Oncol. 9 (2016) 72.
[25] D. Li, T. Han, J. Liao, X. Hu, S. Xu, K. Tian, X. Gu, K. Cheng, Z. Li, H. Hua, J. Xu, Oridonin, a promising *ent*-kaurane diterpenoid lead compound, Int. J. Mol. Sci. 17 (2016) 1395.
[26] D. Li, T. Han, S. Xu, T. Zhou, K. Tian, X. Hu, K. Cheng, Z. Li, H. Hua, J. Xu, Antitumor and antibacterial derivatives of oridonin: a main composition of Dong-Ling-Cao, Molecules 21 (2016) 575.
[27] S. Xu, D. Li, L. Pei, H. Yao, C. Wang, H. Cai, H. Yao, X. Wu, J. Xu, Design, synthesis and antimycobacterial activity evaluation of natural oridonin derivatives, Bioorg. Med. Chem. Lett 24 (2014) 2811–2814.
[28] D. Li, L. Wang, H. Cai, Y. Zhang, J. Xu, Synthesis and biological evaluation of novel furozan-based nitric oxide-releasing derivatives of oridonin as potential anti-tumor agents, Molecules 17 (2012) 7556–7568.
[29] A.K. Steiger, S. Pardue, C.G. Kevil, M.D. Pluth, Self-immolative thiocarbamates provide access to triggered H_2S donors and analyte replacement fluorescent probes, J. Am. Chem. Soc. 138 (2016) 7256–7259.
[30] G.K. Kolluru, X. Shen, S. Yuan, C.G. Kevil, Gasotransmitter heterocellular signaling, Antioxidants Redox Signal. 26 (2017) 936–960.
[31] J.L. Wallace, R. Wang, Hydrogen sulfide-based therapeutics: exploiting a unique but ubiquitous gasotransmitter, Nat. Rev. Drug Discov. 14 (2015) 329–345.
[32] C. Szabo, Gasotransmitters in cancer: from pathophysiology to experimental therapy, Nat. Rev. Drug Discov. 15 (2016) 185–203.
[33] Y. Kimura, Y.I. Goto, H. Kimura, Hydrogen sulfide increases glutathione production and suppresses oxidative stress in mitochondria, Antioxidants Redox Signal. 12 (2010) 1–13.
[34] L. Li, P. Rose, P.K. Moore, Hydrogen sulfide and cell signaling, Annu. Rev. Pharmacol. Toxicol. 51 (2011) 169–187.
[35] Y.H. Liu, M. Lu, L.F. Hu, P.T. Wong, G.D. Webb, J.S. Bian, Hydrogen sulfide in the mammalian cardiovascular system, Antioxidants Redox Signal. 17 (2012) 141–185.
[36] S. Mani, A. Untereiner, L. Wu, R. Wang, Hydrogen sulfide and the pathogenesis of atherosclerosis, Antioxidants Redox Signal. 20 (2014) 805–817.
[37] B.L. Predmore, D.J. Lefer, G. Gojon, Hydrogen sulfide in biochemistry and medicine, Antioxidants Redox Signal. 17 (2012) 119–140.
[38] W.J. Cai, M.J. Wang, P.K. Moore, H.M. Jin, T. Yao, Y.C. Zhu, The novel proangiogenic effect of hydrogen sulfide is dependent on Akt phosphorylation, Cardiovasc. Res. 76 (2007) 29–40.
[39] D.D. Wu, J. Wang, H. Li, M.Z. Xue, A.L. Ji, Y.Z. Li, Role of hydrogen sulfide in ischemia-reperfusion injury, Oxid. Med. Cell Longev. 2015 (2015) 1–16.
[40] A.E. Abdulle, H. van Goor, D.J. Mulder, Hydrogen sulfide: a therapeutic option in systemic sclerosis, Int. J. Mol. Sci. 19 (2018) 4121.
[41] N. Sen, Functional and molecular insights of hydrogen sulfide signaling and protein sulfhydration, J. Mol. Biol. 429 (2017) 543–561.
[42] D. Wu, M. Li, W. Tian, S. Wang, L. Cui, H. Li, H. Wang, A. Ji, Y. Li, Hydrogen sulfide acts as a double-edged sword in human hepatocellular carcinoma cells through EGFR/ERK/MMP-2 and PTEN/AKT signaling pathways, Sci. Rep. 7 (2017) 5134.
[43] S.S. Wang, Y.H. Chen, N. Chen, L.J. Wang, D.X. Chen, H.L. Weng, S. Dooley, H.G. Ding, Hydrogen sulfide promotes autophagy of hepatocellular carcinoma cells through the PI3K/Akt/mTOR signaling pathway, Cell Death Dis. 8 (2017) e2688.
[44] Y. Zhen, W. Zhang, C. Liu, J. He, Y. Lu, R. Guo, J. Feng, Y. Zhang, J. Chen, Exogenous hydrogen sulfide promotes C6 glioma cell growth through activation of the p38 MAPK/ERK1/2-COX-2 pathways, Oncol. Rep. 34 (2015) 2413–2422.
[45] M. Li, J. Li, T. Zhang, Q. Zhao, J. Cheng, B. Liu, Z. Wang, L. Zhao, C. Wang, Syntheses, toxicities and anti-inflammation of H_2S-donors based on non-steroidal anti-inflammatory drugs, Eur. J. Med. Chem. 138 (2017) 51–65.
[46] L. Li, M. Whiteman, Y.Y. Guan, K.L. Neo, Y. Cheng, S.W. Lee, Y. Zhao, R. Baskar, C.H. Tan, P.K. Moore, Characterization of a novel, water-soluble hydrogen sulfide-releasing molecule (GYY4137): new insights into the biology of hydrogen sulfide, Circulation 117 (2008) 2351–2360.
[47] K. Ma, Y. Liu, Q. Zhu, C.H. Liu, J.L. Duan, B.K. Tan, Y.Z. Zhu, H_2S Donor, *S*-propargyl-cysteine, increases CSE in SGC-7901 and cancer-induced mice: evidence for a novel anti-cancer effect of endogenous H_2S? PLoS One 6 (2011), e20525.
[48] Y. Zhao, M.D. Pluth, Hydrogen sulfide donors activated by reactive oxygen species, Angew. Chem. Int. Ed. 55 (2016) 14638–14642.
[49] Y. Zhao, S.G. Bolton, M.D. Pluth, Light-activated COS/H_2S donation from photocaged thiocarbamates, Org. Lett. 19 (2017) 2278–2281.
[50] J.L. Wallace, G. Caliendo, V. Santagada, G. Cirino, Markedly reduced toxicity of a hydrogen sulphide-releasing derivative of naproxen (ATB-346), Br. J. Pharmacol. 159 (2010) 1236–1246.
[51] M. Chattopadhyay, R. Kodela, K.R. Olson, K. Kashfi, NOSH-aspirin (NBS-1120),

a novel nitric oxide- and hydrogen sulfide-releasing hybrid is a potent inhibitor of colon cancer cell growth in vitro and in a xenograft mouse model, Biochem. Biophys. Res. Commun. 419 (2012) 523–528.
[52] M. Chattopadhyay, R. Kodela, N. Nath, A. Barsegian, D. Boring, K. Kashfi, Hydrogen sulfide-releasing aspirin suppresses NF-κB signaling in estrogen receptor negative breast cancer cells in vitro and in vivo, Biochem. Pharmacol. 83 (2012) 723–732.
[53] B. Szczesny, K. Modis, K. Yanagi, C. Coletta, S. Le Trionnaire, A. Perry, M.E. Wood, M. Whiteman, C. Szabo, AP39, a novel mitochondria-targeted hydrogen sulfide donor, stimulates cellular bioenergetics, exerts cytoprotective effects and protects against the loss of mitochondrial DNA integrity in oxidatively stressed endothelial cells in vitro, Nitric Oxide 41 (2014) 120–130.
[54] J. Frantzias, J.G. Logan, P. Mollat, A. Sparatore, P. Del Soldato, S.H. Ralston, A.I. Idris, Hydrogen sulphide-releasing diclofenac derivatives inhibit breast cancer-induced osteoclastogenesis in vitro and prevent osteolysis ex vivo, Br. J. Pharmacol. 165 (2012) 1914–1925.
[55] G. Caliendo, G. Cirino, V. Santagada, J.L. Wallace, Synthesis and biological effects of hydrogen sulfide (H_2S): development of H_2S-releasing drugs as pharmaceuticals, J. Med. Chem. 53 (2010) 6275–6286.
[56] U. Hasegawa, N. Tateishi, H. Uyama, A.J. van der Vlies, Hydrolysis-sensitive dithiolethione prodrug micelles, Macromol. Biosci. 15 (2015) 1512–1522.
[57] H. Li, X. Gao, X. Huang, X. Wang, S. Xu, T. Uchita, M. Gao, J. Xu, H. Hua, D. Li, Hydrogen sulfide donating *ent*-kaurane and spirolactone-type 6,7-*seco*-*ent*-kaurane derivatives: design, synthesis and antiproliferative properties, Eur. J. Med. Chem. 178 (2019) 446–457.
[58] X. Hu, R. Jiao, H. Li, X. Wang, H. Lyu, X. Gao, F. Xu, Z. Li, H. Hua, D. Li, Antiproliferative hydrogen sulfide releasing evodiamine derivatives and their apoptosis inducing properties, Eur. J. Med. Chem. 151 (2018) 376–388.
[59] T. Han, J. Li, J. Xue, H. Li, F. Xu, K. Cheng, D. Li, Z. Li, M. Gao, H. Hua, Scutellarin derivatives as apoptosis inducers: design, synthesis and biological evaluation, Eur. J. Med. Chem. 135 (2017) 270–281.
[60] D.C. Altieri, Survivin and IAP proteins in cell-death mechanisms, Biochem. J. 430 (2010) 199–205.
[61] C. Sun, G. Dotti, B. Savoldo, Utilizing cell-based therapeutics to overcome immune evasion in hematologic malignancies, Blood 127 (2016) 3350–3359.
[62] F. Xu, X. Gao, H. Li, S. Xu, X. Li, X. Hu, Z. Li, J. Xu, H. Hua, D. Li, Hydrogen sulfide releasing enmein-type diterpenoid derivatives as apoptosis inducers through mitochondria-related pathways, Bioorg. Chem. 82 (2018) 192–203.
[63] T. Han, K. Tian, H. Pan, Y. Liu, F. Xu, Z. Li, T. Uchita, M. Gao, H. Hua, D. Li, Novel hybrids of brefeldin A and nitrogen mustards with improved antiproliferative selectivity: design, synthesis and antitumor biological evaluation, Eur. J. Med. Chem. 150 (2018) 53–63.
[64] S.Y. Wu, A.T.H. Wu, S.H. Liu, MicroRNA-17-5p regulated apoptosis-related protein expression and radiosensitivity in oral squamous cell carcinoma caused by betel nut chewing, Oncotarget 7 (2016) 51482–51493.